

In the format provided by the authors and unedited.

Salinomycin kills cancer stem cells by sequestering iron in lysosomes

Trang Thi Mai^{1,2,3,4,9}, Ahmed Hamai^{5,9}, Antje Hienzsch^{4,6,9}, Tatiana Cañeque^{1,2,3,4}, Sebastian Müller^{1,2,3}, Julien Wicinski⁷, Olivier Cabaud⁷, Christine Leroy⁵, Amandine David⁵, Verónica Acevedo^{1,2,3}, Akihide Ryo⁸, Christophe Ginestier⁷, Daniel Birnbaum⁷, Emmanuelle Charafe-Jauffret⁷, Patrice Codogno⁵, Maryam Mehrpour^{5*}, Raphaël Rodriguez^{1,2,3,4,*}

¹ Institut Curie, PSL Research University, Chemical Cell Biology group, 26 rue d'Ulm, 75248 Paris Cedex 05, France.

² CNRS UMR3666, 75005 Paris, France.

³ INSERM U1143, 75005 Paris, France.

⁴ Institut de Chimie des Substances Naturelles, UPR2301, 1 Avenue de la Terrasse, 91198 Gif-sur-Yvette Cedex, France.

⁵ Institut Necker-Enfants Malades, INSERM U1151-CNRS UMR8253, 14 rue Maria Helena Vieira Da Silva, 75993 Paris Cedex 14, France.

⁶ ABX advanced biochemical compounds, Heinrich-Glaeser-Str. 10-14, D-01454 Radeberg, Germany.

⁷ Aix Marseille Université, CNRS, INSERM, Institut Paoli-Calmettes, CRCM, Equipe Oncologie Moléculaire labellisée 'Ligue contre le cancer', Marseille, France.

⁸ Department of Microbiology, Yokohama City University School of Medicine, Yokohama 236-0004, Japan.

⁹ These authors contributed equally to this work.

* Correspondence should be addressed to R.R. (raphael.rodriguez@curie.fr) and M.M. (maryam.mehrpour@inserm.fr).

Table of contents

Chemical Synthesis

General information	3
Experimental procedures	3
NMR spectra of AM5 and AM4	6

Material and Methods

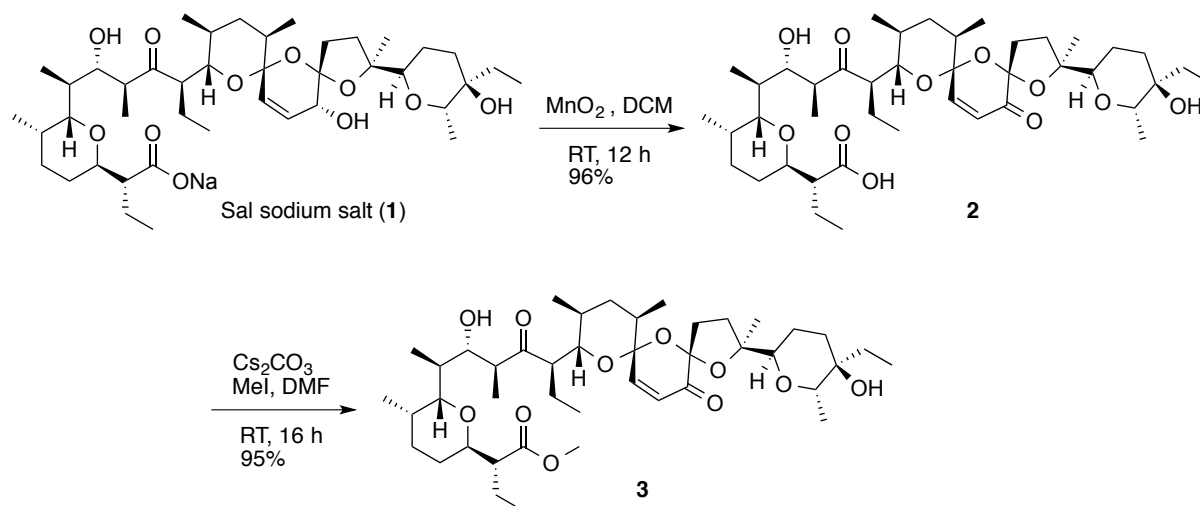
Cell culture	12
Cell viability assay	12
Clonogenic assay	12
Tumorsphere assay	12
Xenograft tumor formation	12
Patient derived xenografts (PDXs)	13
Aldefluor assay	13
Limiting dilution assay	13
Estimation of number of CSCs <i>in vivo</i>	14
Histology	14
Immunoblotting	14
Intracellular sodium measurements	14
Acridine orange (AO) assay	14
Localization of intracellular iron(II)	15
Perls' reaction	15
Lysosomal membrane permeabilization assay	15
Annexin V-FITC/PI assay	15
Lipid ROS measurements	15
Intracellular GSH levels quantification	16
RhoNox-1 reduction assay	16
Electrothermal atomic absorption spectrometry	16
Small interfering RNA transfection	16
RNA extraction and analysis	16
Statistical analysis	16

Supplementary Figures

Supp. Fig. 1.	Molecular structures of synthetic derivatives of Sal	17
Supp. Fig. 2	Sal and AM5 selectively target breast CSCs over primary breast cells	18
Supp. Fig. 3.	AM5 targets CSCs <i>in vitro</i>	20
Supp. Fig. 4.	AM5 reduces MCF-7 tumor growth	21
Supp. Fig. 5.	AM5 targets CSCs <i>in vivo</i> at non-toxic doses	22
Supp. Fig. 6.	Salinomycin derivatives accumulate quantitatively in lysosomes	23
Supp. Fig. 7.	Sal derivatives colocalize with the lysosomal markers Rab7 and Lamp1	24
Supp. Fig. 8.	Sal and AM5 do not alter the lysosomal pH	26
Supp. Fig. 9.	AM5 enters cells independently of endocytosis	27
Supp. Fig. 10.	Labeled AM5 does not colocalize with markers of the ER, mitochondria or Golgi	28
Supp. Fig. 11.	Ferritin co-localizes with lysotracker in cells treated with Sal or AM5	30
Supp. Fig. 12.	Sal and AM5 sequester iron in lysosomes	31
Supp. Fig. 13.	Sal interacts with iron(II) in solution	33
Supp. Fig. 14.	Sal and AM5 induce the production of ROS in HMLER CD24 ^{low} cells	34
Supp. Fig. 15.	Sal and AM5 induce biochemical features characteristic of ferroptosis	35
Supp. Fig. 16.	Cell death can be rescued by cathepsin B inhibition, ROS scavenging and iron chelation	37
Supp. Fig. 17.	Preferential uptake of transferrin by ALDH ⁺ iCSCL-10A2 CSCs	39

Chemical Synthesis

General information. All starting materials were purchased from Sigma Aldrich unless stated otherwise and used without further purification, or purified according to *Purification of Laboratory Chemicals* (Armarego, W.L.F., Chai, C.L.L. 5th edition). Solvents were dried under standard conditions. Salinomycin (Sal) technical grade (~12%, Salcox 120) was extracted with dichloromethane and purified by preparative HPLC. Reactions were monitored by thin layer chromatography using aluminium-baked plates from Merck (60 F254). TLC plates were visualized with UV light and/or by treatment with cerium molybdate solution and heating. Reaction products were purified using regular column chromatography (Merck silica gel 60, 0.040-0.063 mm; 230-400 mesh), a PuriFlash 430 system (Interchim) fitted with pre-packed silica gel columns (PuriFlash or GraceResolv, 4-120 g columns, 50 μ m particle size), or a Spot Prep II system (Armen Instrument) fitted with a Merck Millipore reversed phase column (Purospher® RP-18 LiChroCART® 250-10). NMR spectroscopy was performed on Bruker 300 and 500 MHz apparatuses equipped with cryoprobes. Titration of Sal and AM5 with iron were monitored on a Bruker 600 MHz equipped with a MicroProbe. Spectra were run in CD₃OD, CD₃CN or CDCl₃ at 298 K unless stated otherwise. Molecular structures were characterized using a comprehensive dataset including ¹H and ¹³C NMR spectra (1D and 2D experiments including COSY, NOESY, HMBC, HSQC). ¹H chemical shifts δ are expressed in ppm using the residual non-deuterated solvent as internal standard and the coupling constants *J* are specified in Hz. The following abbreviations are used: s, singlet; d, doublet; dd, double doublet; t, triplet; q, quartet; m, multiplet; bs, broad singlet. ¹³C chemical shifts are expressed in ppm using the residual non-deuterated solvent as internal standard. Exact masses were recorded on a LCT Premier XE (Waters) equipped with an ESI ionization source and a TOF detector.

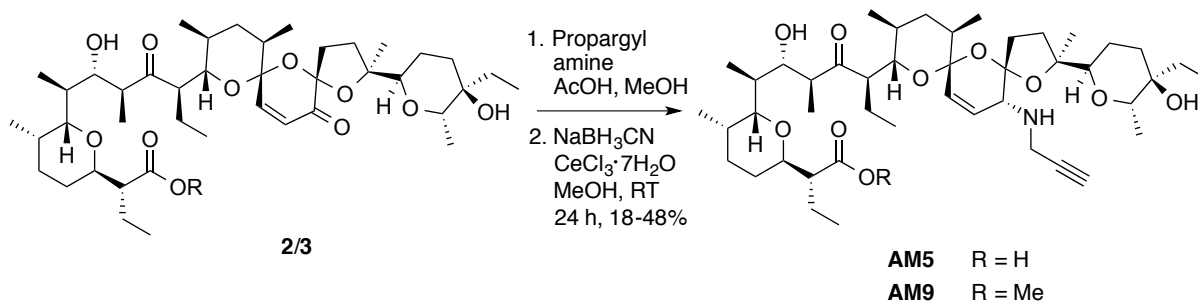


Synthesis of 2. The sodium salt of salinomycin **1** (2.0 g, 2.6 mmol) was dissolved in dichloromethane (250 mL) prior to addition of manganese dioxide (9.0 g, 103.5 mmol, 40 eq.). The suspension was stirred overnight at room temperature (RT) and filtrated over celite. The filtrate was washed with an aq. soln. of H₂SO₄ (15 mM), dried over MgSO₄ and concentrated under reduced pressure to yield **2** (1.7 g, 2.3 mmol, 96%) as a white solid, which was used without further purification. ¹H NMR (CDCl₃, 500 MHz) δ 0.64-0.72 (6H, m), 0.72-0.82 (6H, m), 0.83-0.98 (12H, m), 1.04-1.17 (4H, m), 1.19-1.27 (2H, m), 1.30-1.57 (12H, m), 1.59-2.05 (14H, m), 2.43-2.60 (2H, m), 2.63-2.73 (1H, m) 2.76-2.88 (1H, m), 3.38-3.52 (1H, m), 3.66 (1H, d, *J* = 9.6 Hz), 3.76 (1H, d, *J* = 10.2 Hz), 3.88-4.04 (2H, m), 4.11-4.22 (1H, m),

6.20 (1H, d, $J = 10.7$ Hz), 7.12 (1H, d, $J = 10.7$ Hz). ^{13}C NMR (CDCl_3 , 125 MHz) δ 6.6, 7.0, 11.3, 12.1, 12.6, 13.1, 14.2, 15.5, 16.0, 17.6, 19.8, 20.7, 22.9, 26.4, 27.2, 28.3, 28.6, 32.1, 32.2, 33.2, 34.2, 35.5, 38.4, 40.2, 50.3, 51.6, 55.7, 67.7, 69.6, 71.0, 73.2, 75.8, 76.5, 76.7, 90.0, 98.0, 105.3, 127.1, 142.3, 183.2, 187.9, 217.9. HRMS (ESI) m/z : Calculated for $\text{C}_{42}\text{H}_{68}\text{NaO}_{11}^+$ [$\text{M}+\text{Na}^+$] 771.4654, found: 771.4660.

Synthesis of 3. In a dry Schlenk tube flushed with argon, **2** (100 mg, 0.13 mmol) was dissolved in anhydrous dimethylformamide (3 mL). Cesium carbonate (56.5 mg, 0.17 mmol, 1.3 eq.) was added followed by methyl iodide (11 μL , 0.17 mmol, 1.3 eq.) and the reaction mixture was stirred for 24 h at RT. After completion of the reaction, the solvent was removed under reduced pressure and the residue was taken up in dichloromethane. The solution was washed with an aq. soln. of H_2SO_4 (15 mM), a sat. aq. soln. of NaHCO_3 , water and brine, then dried over MgSO_4 . The solution was filtrated, concentrated under reduced pressure and purified on silica gel using the PuriFlash system (dichloromethane/methanol 9.8:0.2) to give **3** (96.5 mg, 0.13 mmol, 95%) as a white foam. ^1H NMR (CDCl_3 , 300 MHz) δ 0.63-0.72 (9H, m), 0.72-0.77 (3H, d, $J = 7.0$ Hz), 0.80-0.89 (12H, m), 1.06-1.17 (7H, m), 1.17-1.21 (2H, m), 1.21-1.32 (3H, m), 1.32-1.46 (8H, m), 1.46-1.58 (3H, m), 1.60-1.80 (4H, m), 1.80-1.94 (2H, m), 1.98-2.12 (2H, m), 2.48-2.56 (1H, m), 2.58-2.68 (1H, m), 2.81-2.99 (2H, m), 3.26-3.32 (1H, m), 3.51 (1H, dd, $J = 9.8, 1.5$ Hz), 3.59-3.73 (2H, m), 3.70 (3H, s), 3.85-3.97 (2H, m), 6.16 (1H, d, $J = 10.7$ Hz), 7.18 (1H, d, $J = 10.7$ Hz). ^{13}C NMR (CDCl_3 , 125 MHz) δ 6.6, 7.2, 11.1, 11.9, 12.1, 14.0, 15.0, 17.9, 18.7, 19.8, 20.8, 22.6, 22.7, 26.3, 28.1, 29.2, 29.7, 30.3, 34.26, 34.30, 34.4, 36.6, 39.2, 39.9, 47.7, 49.1, 52.7, 57.5, 70.0, 71.2, 71.8, 72.3, 75.1, 77.1, 77.4, 88.7, 97.6, 105.5, 127.3, 144.2, 176.6, 190.9, 214.3. HRMS (ESI) m/z : calculated for $\text{C}_{43}\text{H}_{70}\text{NaO}_{11}^+$ [$\text{M}+\text{Na}^+$] 785.4810, found: 785.4807.

Reductive amination of **2** and **3**.



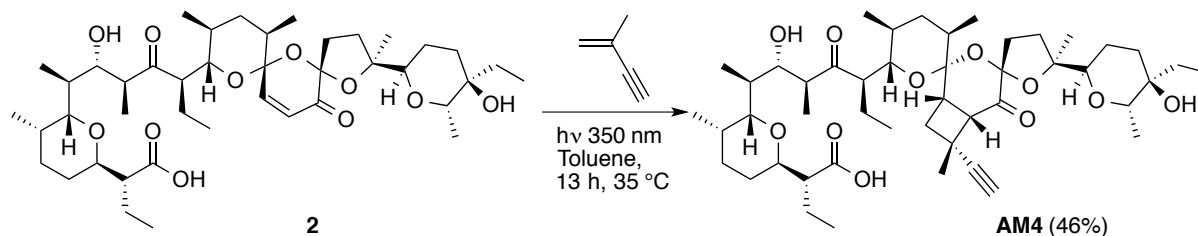
Intermediate **2** (or **3**) (100 mg, ~ 0.13 mmol) was dissolved in methanol (5 mL) followed by the addition of the relevant primary amine (10.0 eq.) and acetic acid (50 μL). The solution was stirred 1 h at RT prior to addition of $\text{CeCl}_3 \cdot 7\text{H}_2\text{O}$ (50 mg, 1.0 eq.), and the dropwise addition of a soln. of NaBH_3CN (11.7 mg, 1.4 eq., 2 mL of methanol) over 8 h at RT using a syringe pump. The reaction mixture was quenched with an aq. soln. of H_2SO_4 (15 mM) and extracted with dichloromethane. The aqueous layer was extracted twice with dichloromethane and the combined organic layers were washed with an aq. soln. of H_2SO_4 (15 mM), a sat. aq. soln. of NaHCO_3 , water and brine. The organic phase was dried over MgSO_4 and concentrated under reduced pressure. The product was purified by flash chromatography on silica gel or using a PuriFlash system (dichloromethane/methanol 9.6:0.4), then by HPLC equipped with a C_{18} -reverse phase column (gradient acetonitrile/water/formic acid 1:1:0.1 to acetonitrile/formic acid 1:0.1).

Synthesis of AM5. **AM5** was obtained as a colorless foam (46 mg, 0.06 mmol, 44%) from **2** (103 mg, 0.13 mmol), propargyl amine (86 μL , 1.34 mmol, 10.0 eq.), NaBH_3CN (11 mg, 0.17 mmol, 1.3 eq.), $\text{CeCl}_3 \cdot 7\text{H}_2\text{O}$ (50 mg, 0.13 mmol, 1.0 eq.) and acetic acid (50 μL in 7 mL of

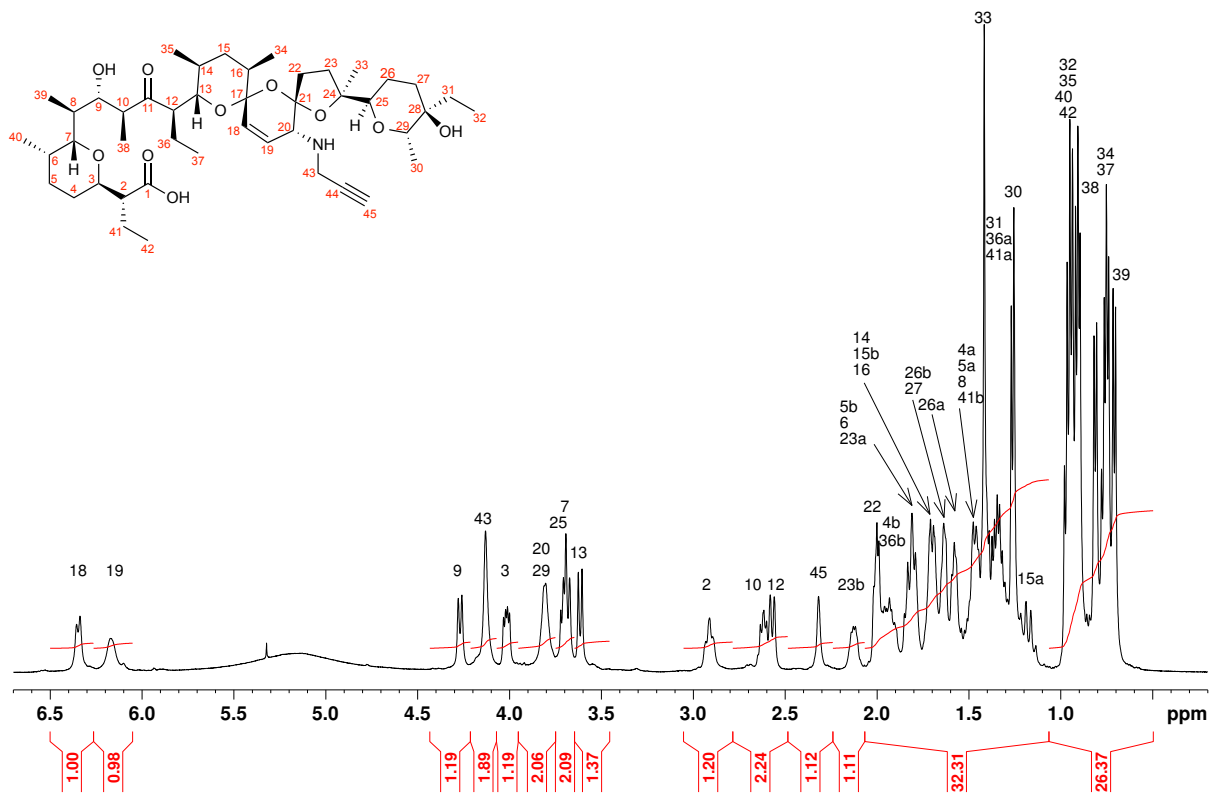
MeOH). ^1H NMR (CDCl_3 , 500 MHz, 278 K) δ 0.69 (3H, d, $J = 6.9$ Hz), 0.71-0.77 (6H, m), 0.79 (3H, d, $J = 7.2$ Hz), 0.86-0.97 (12H, m), 1.16 (1H, q, $J = 14.0$), 1.24 (3H, d, $J = 7.4$ Hz), 1.26-1.38 (4H, m), 1.38-1.42 (3H, m), 1.42-1.52 (4H, m), 1.52-1.59 (1H, m), 1.59-1.64 (3H, m), 1.64-1.74 (3H, m), 1.74-1.85 (3H, m), 1.85-2.02 (4H, m), 2.06-2.16 (1H, m), 2.30 (1H, s), 2.51-2.64 (2H, m), 2.89 (1H, td, $J = 11.3, 3.9$ Hz), 3.60 (1H, d, $J = 10.2$ Hz), 3.62-3.72 (2H, m), 3.73-3.84 (2H, m), 4.00 (1H, dd, $J = 11.1, 5.7$ Hz), 4.11 (2H, s), 4.25 (1H, d, $J = 10.1$ Hz), 6.15 (1H, s), 6.33 (1H, d, $J = 10.1$ Hz). ^{13}C NMR (125 MHz, CDCl_3 , 278 K) δ 6.6, 7.1, 11.2, 12.3, 12.6, 13.4, 14.4, 15.8, 16.3, 17.8, 20.0, 22.0, 23.2, 25.5, 26.6, 28.2, 28.9, 29.8, 30.6, 30.9, 32.4, 36.2, 36.7, 38.0, 39.5, 40.1, 48.9, 50.2, 52.7, 55.5, 68.0, 71.1, 71.6, 73.3, 74.3, 75.1, 75.6, 77.0, 88.4, 98.2, 105.7, 127.3, 128.4, 179.6, 214.6. HRMS (ESI) m/z : Calculated for $\text{C}_{45}\text{H}_{74}\text{NO}_{10}^+$ [$\text{M}+\text{H}^+$] 788.5307, found: 788.5304.

Synthesis of AM9. AM9 was obtained as a colorless foam (54 mg, 0.07 mmol, 48%) from **3** (106 mg, 0.14 mmol), propargyl amine (89 μL , 1.39 mmol, 10.0 eq.), NaBH_3CN (9.6 mg, 0.15 mmol, 1.1 eq.), $\text{CeCl}_3 \cdot 7\text{H}_2\text{O}$ (52 mg, 0.14 mmol, 1.0 eq.) and acetic acid (50 μL in 7 mL of MeOH). ^1H NMR (CDCl_3 , 500 MHz, 278 K) δ 0.72 (3H, d, $J = 6.9$ Hz), 0.75-0.87 (11H, m), 0.88-0.99 (9H, m), 1.07 (1H, ddd, $J = 13.0, 13.0, 12.0$ Hz), 1.20-1.68 (22H, m), 1.70-2.05 (9H, m), 2.10-2.26 (3H, m), 2.30-2.41 (2H, m), 2.69-2.74 (1H, m), 3.04 (1H, dt, $J = 10.8, 4.1$ Hz), 3.47-3.72 (4H, m), 3.80-3.88 (1H, m), 3.90 (3H, s), 4.02-4.09 (2H, m), 6.01-6.08 (2H, m). ^{13}C NMR (CDCl_3 , 125 MHz, 278 K) δ 6.5, 7.4, 11.0, 12.0, 13.2, 13.9, 14.7, 15.7, 17.5, 19.7, 22.2, 22.7, 25.5, 26.2, 28.0, 29.0, 30.6, 30.7, 32.9, 36.4, 37.1 (2C), 38.6, 38.7, 40.3, 48.0, 48.6, 52.6, 55.2, 56.6, 69.2, 71.0, 71.7, 73.9, 75.1, 76.9, 77.3, 80.1, 88.0, 98.6, 102.0, 108.3, 123.2, 130.5, 176.2, 214.0. HRMS (ESI) m/z : calculated for $\text{C}_{46}\text{H}_{76}\text{NO}_{10}^+$ [$\text{M}+\text{H}^+$] 802.5464, found: 802.5465.

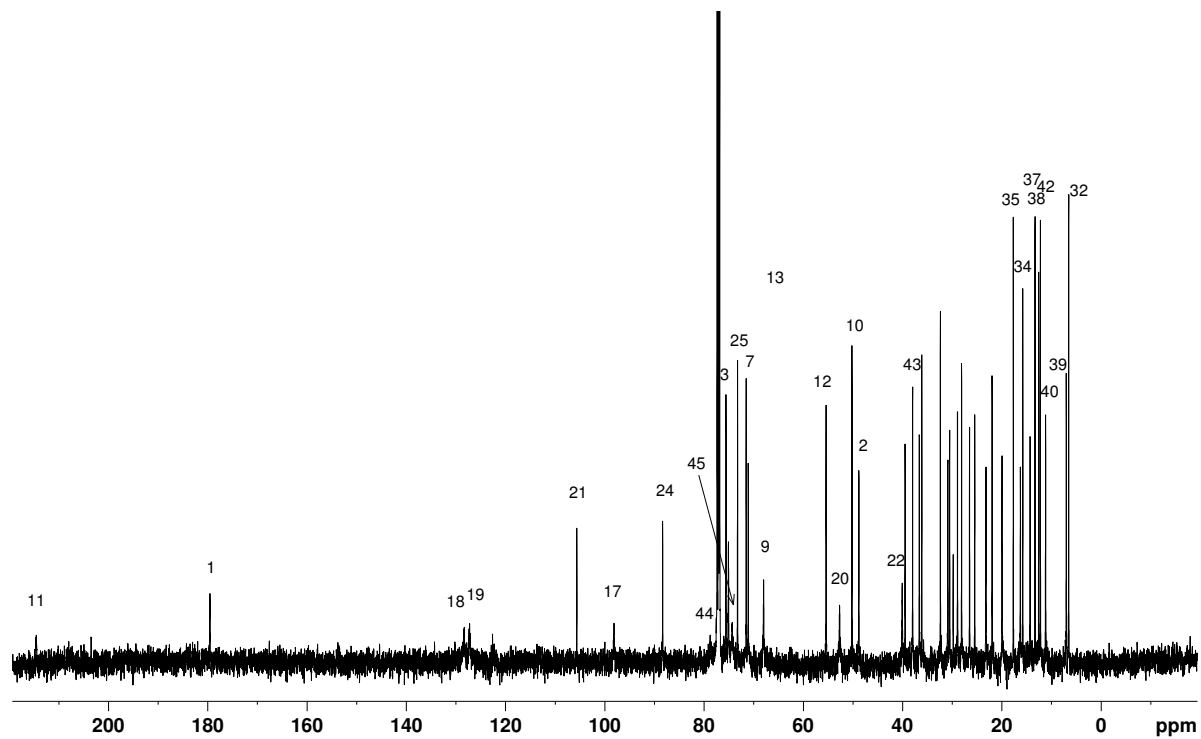
Photocycloaddition.



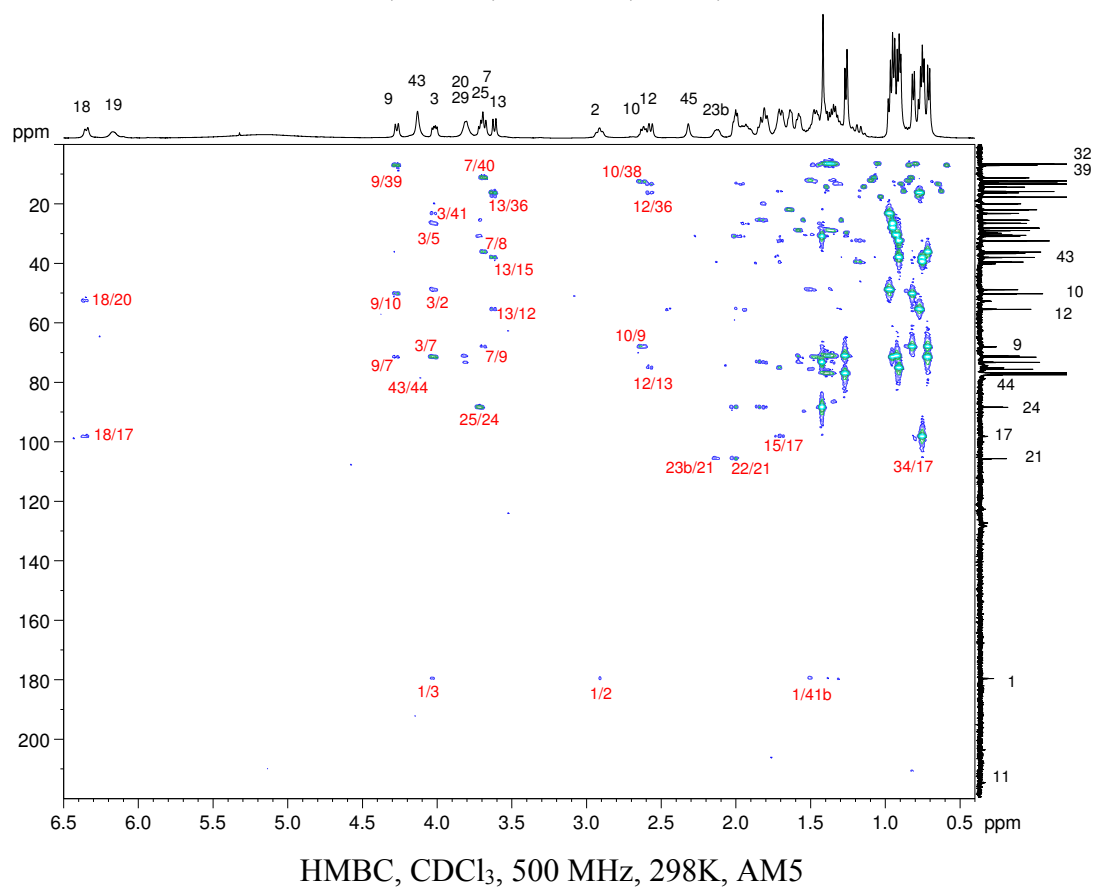
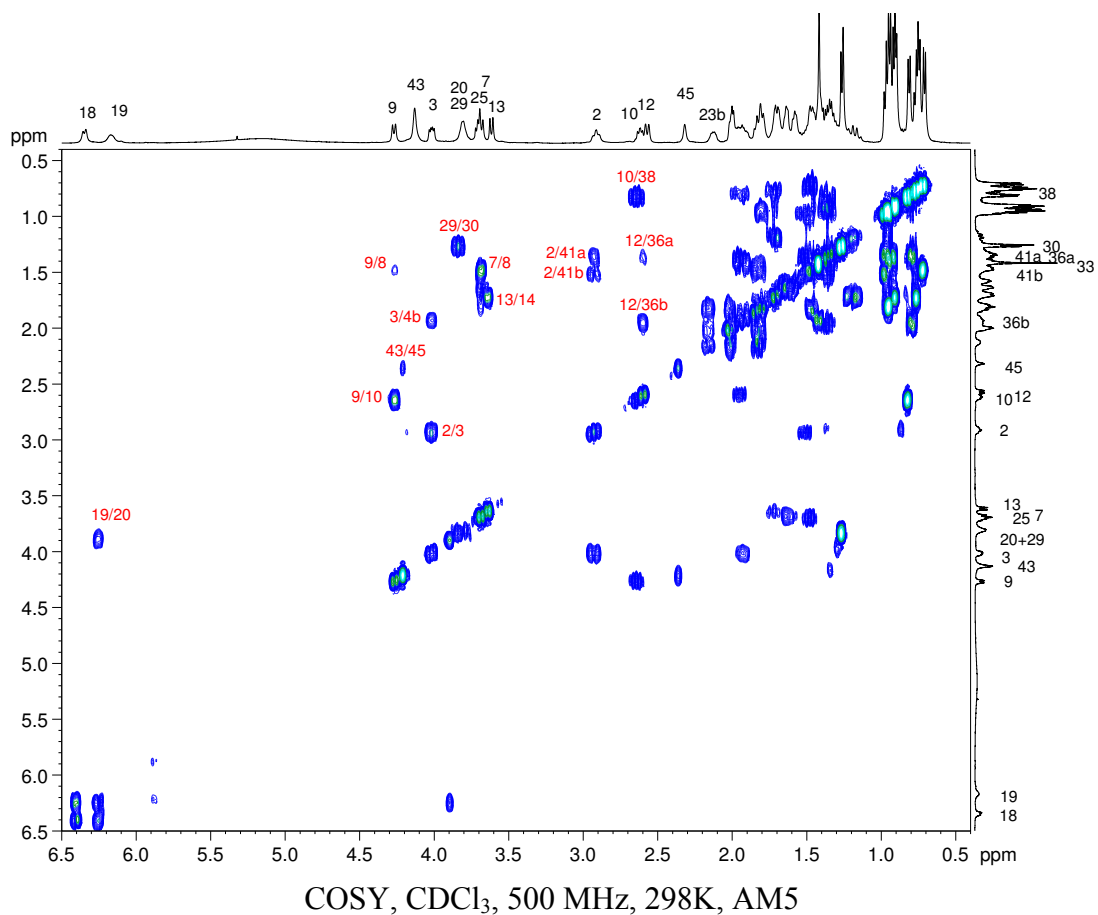
In a dry quartz-vial flushed with argon, intermediate **2** (300 mg, 0.39 mmol) was dissolved in anhydrous toluene (4 mL). 2-Methyl-1-buten-3-yne (380 μL , 10.0 eq.) was added and the solution was exposed to light at 350 nm for 12 h at 35 °C using a Rayonet reactor®. After full conversion of the starting material, the solution was concentrated and purified by flash chromatography on silica gel (dichloromethane/methanol 9.9:0.1 to 9.7:0.3) to give **AM4** (146 mg, 0.18 mmol, 46%, $R_f = 0.28$ using dichloromethane/methanol 9.7:0.3) as a white foam. ^1H NMR (CDCl_3 , 500 MHz, 278 K) δ 0.60-0.74 (6H, m), 0.78 (3H, d, $J = 7.0$ Hz), 0.87-0.99 (12H, m), 1.07 (4H, d, 7.4 Hz), 1.16-1.29 (4H, m), 1.29-1.51 (12H, m), 1.51-1.60 (1H, m), 1.60-1.73 (2H, m), 1.74-1.86 (4H, m), 1.87-2.10 (6H, m), 2.13-2.30 (5H, m), 2.34-2.48 (2H, m), 2.59-2.71 (1H, m), 2.75-2.94 (2H, m), 3.26-3.42 (2H, m), 3.42-3.52 (1H, m), 3.59 (1H, d, $J = 9.5$ Hz), 3.70 (1H, d, $J = 9.5$ Hz), 3.78-3.92 (1H, m), 4.02 (1H, dd, $J = 10.9$ Hz, 6.1 Hz), 4.06-4.22 (1H, m). ^{13}C NMR (CDCl_3 , 125 MHz, 298 K) δ 6.6, 7.0, 10.8, 12.2, 12.9, 13.1, 14.4, 16.4, 18.6 (2C), 19.6, 20.6, 22.2, 22.7, 26.2, 27.9, 29.0, 29.5, 30.1, 30.9, 32.4, 35.4, 35.7 (2C), 35.9, 36.5, 37.5, 39.1, 48.3, 48.4, 48.6, 49.6, 55.1, 67.7, 71.7, 72.2, 72.7, 74.7, 75.0, 76.6, 87.1, 89.5, 100.1, 106.4, 178.3, 211.1, 213.5. HRMS (ESI) m/z : calculated for $\text{C}_{47}\text{H}_{74}\text{NaO}_{11}^+$ [$\text{M}+\text{Na}^+$] 837.5123, found: 837.5115.

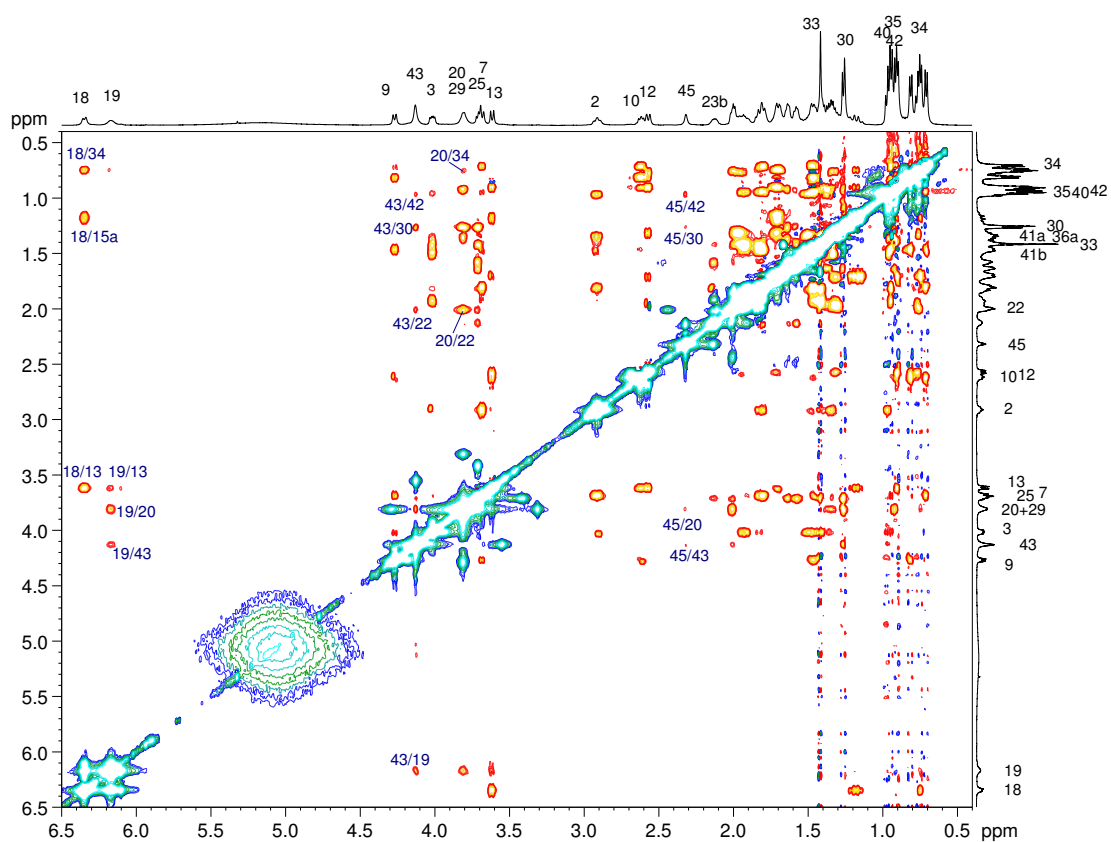
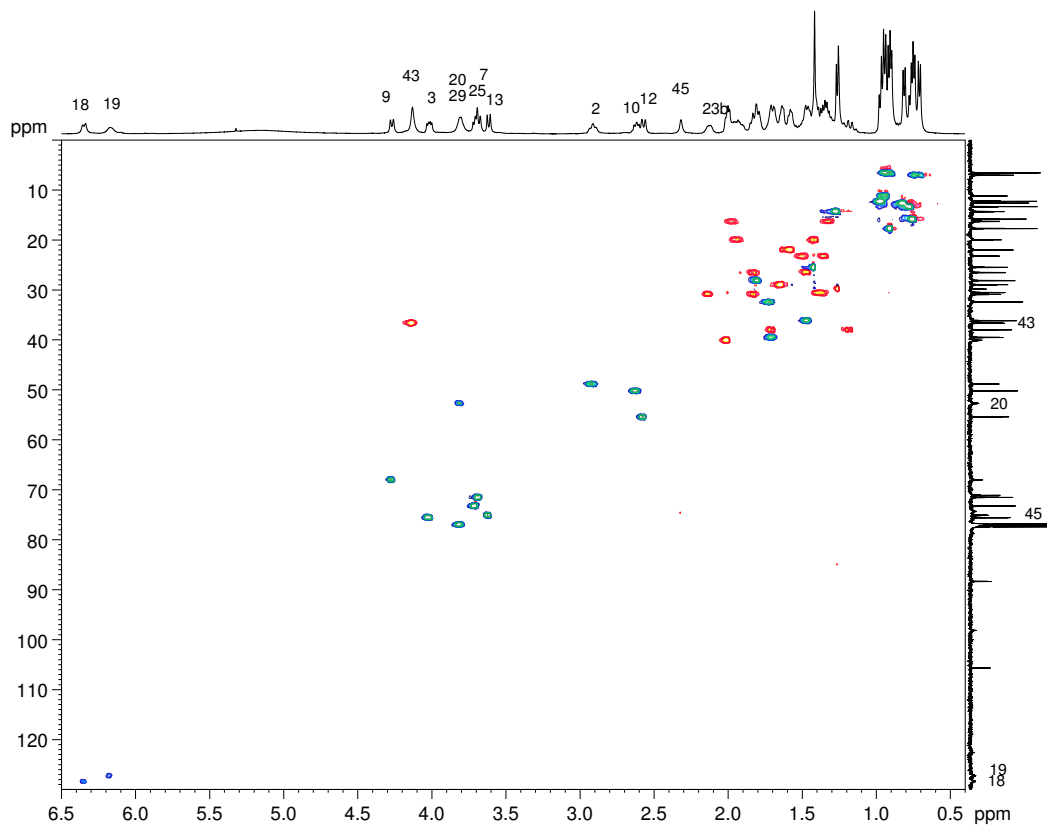


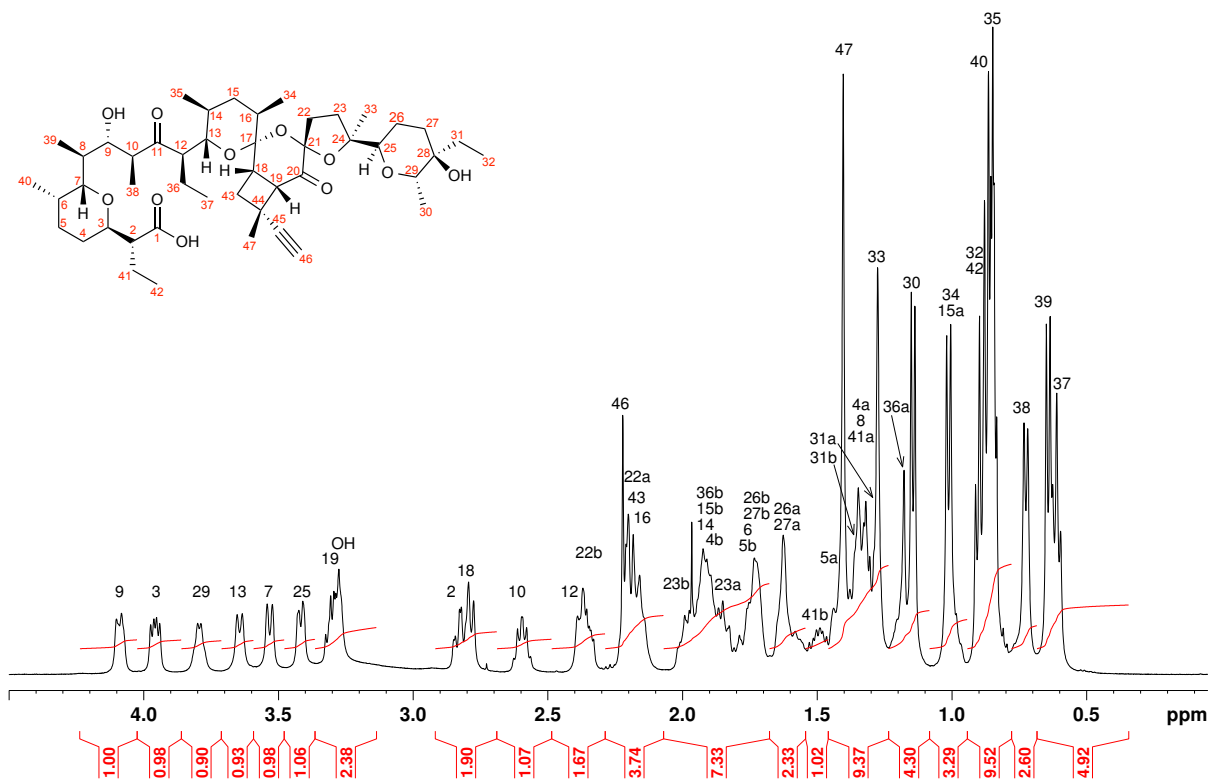
¹H-NMR, CDCl₃, 500 MHz, 298K, AM5



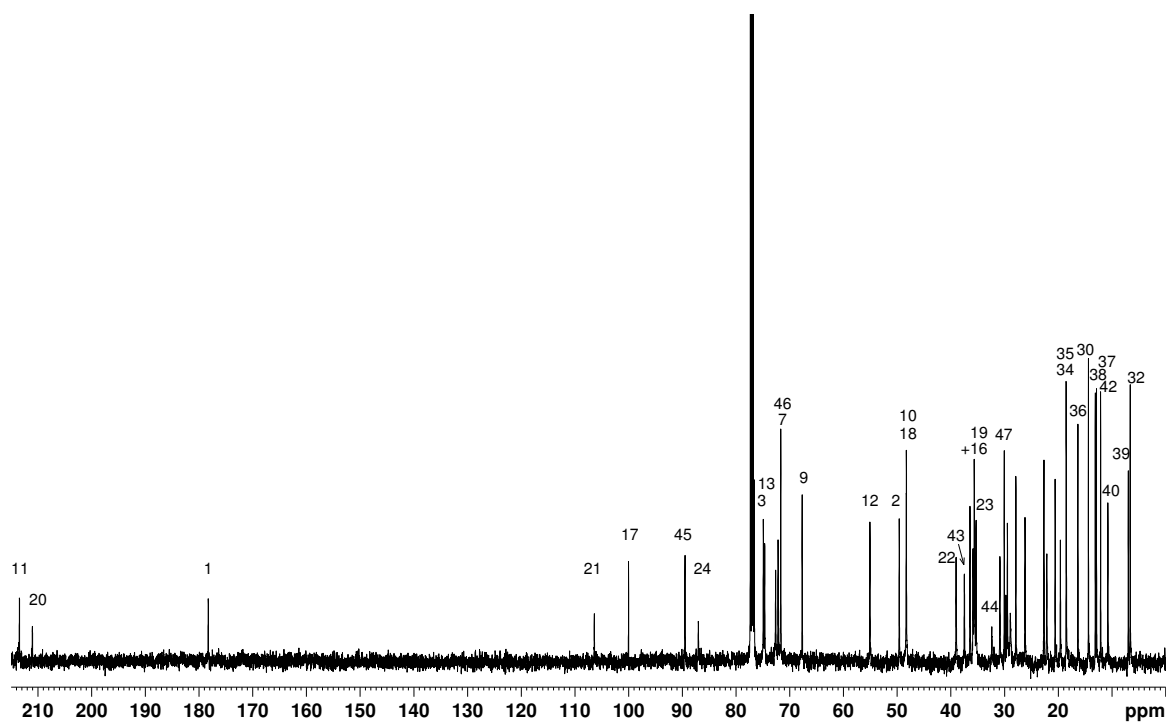
¹³C-NMR, CDCl₃, 500 MHz, 298K, AM5



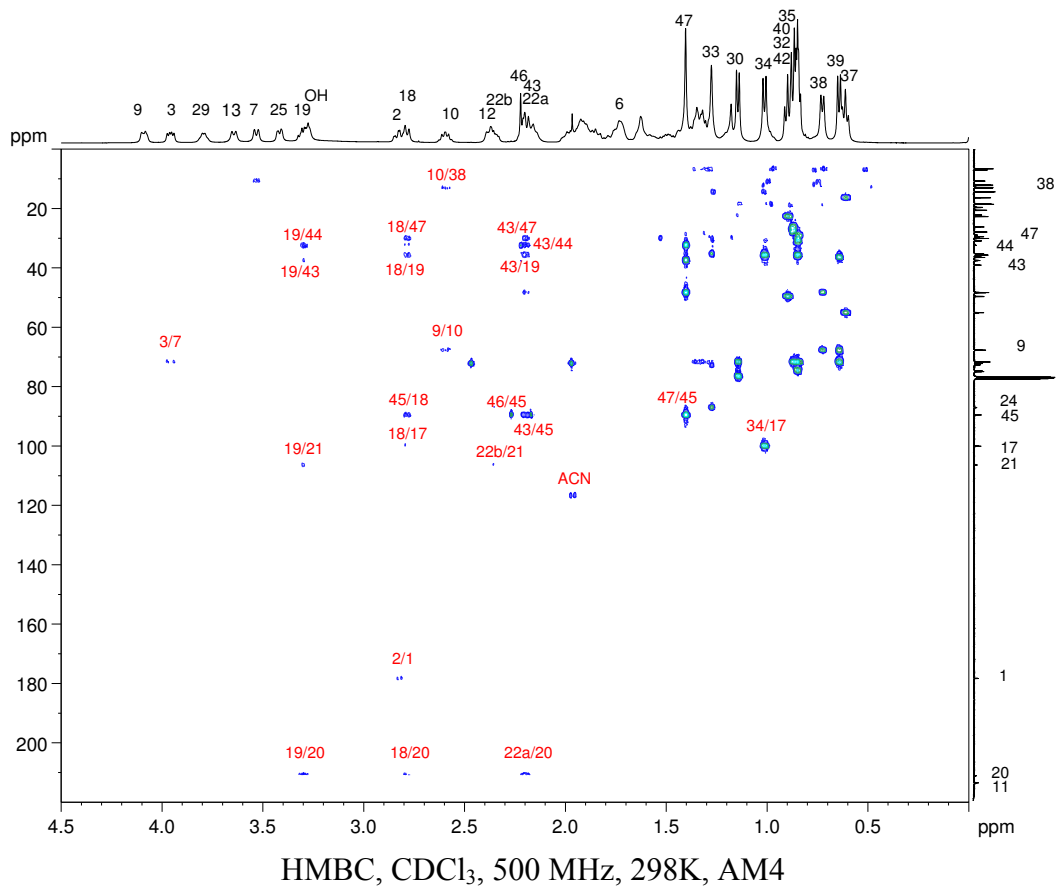
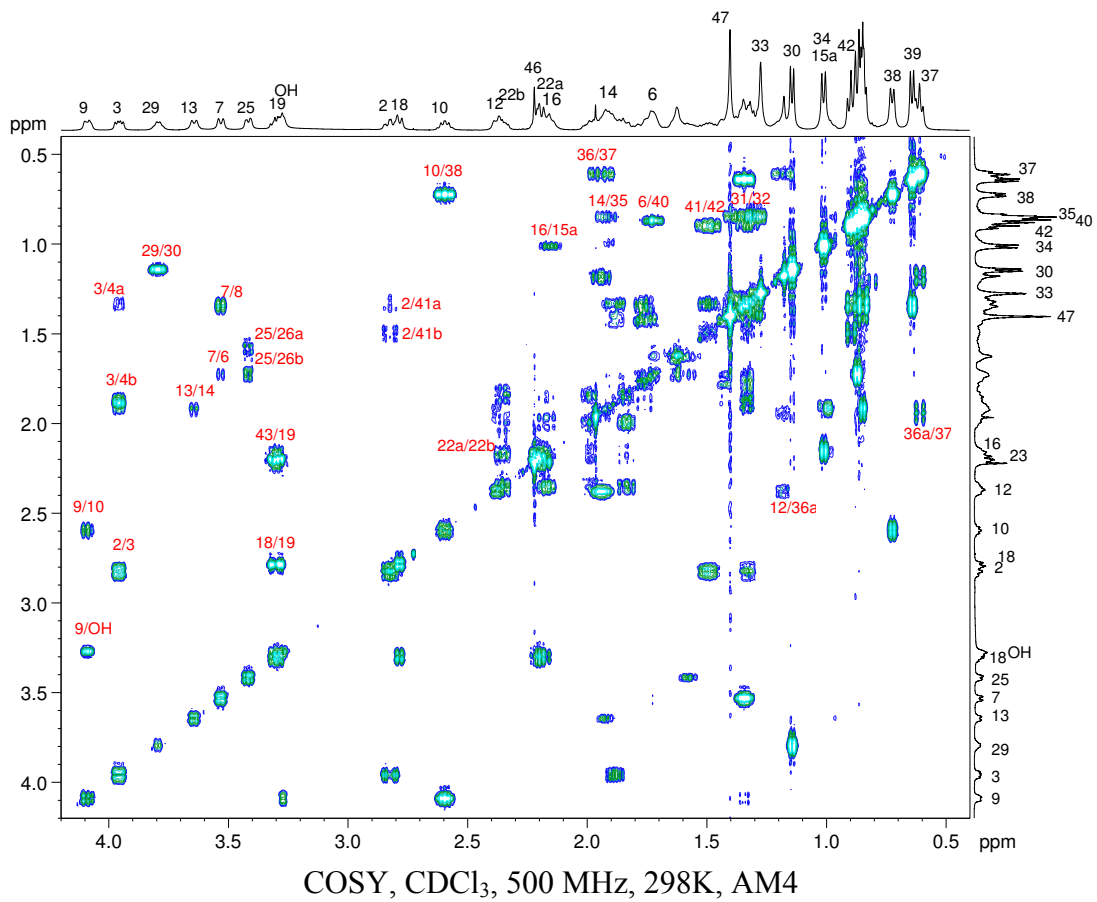


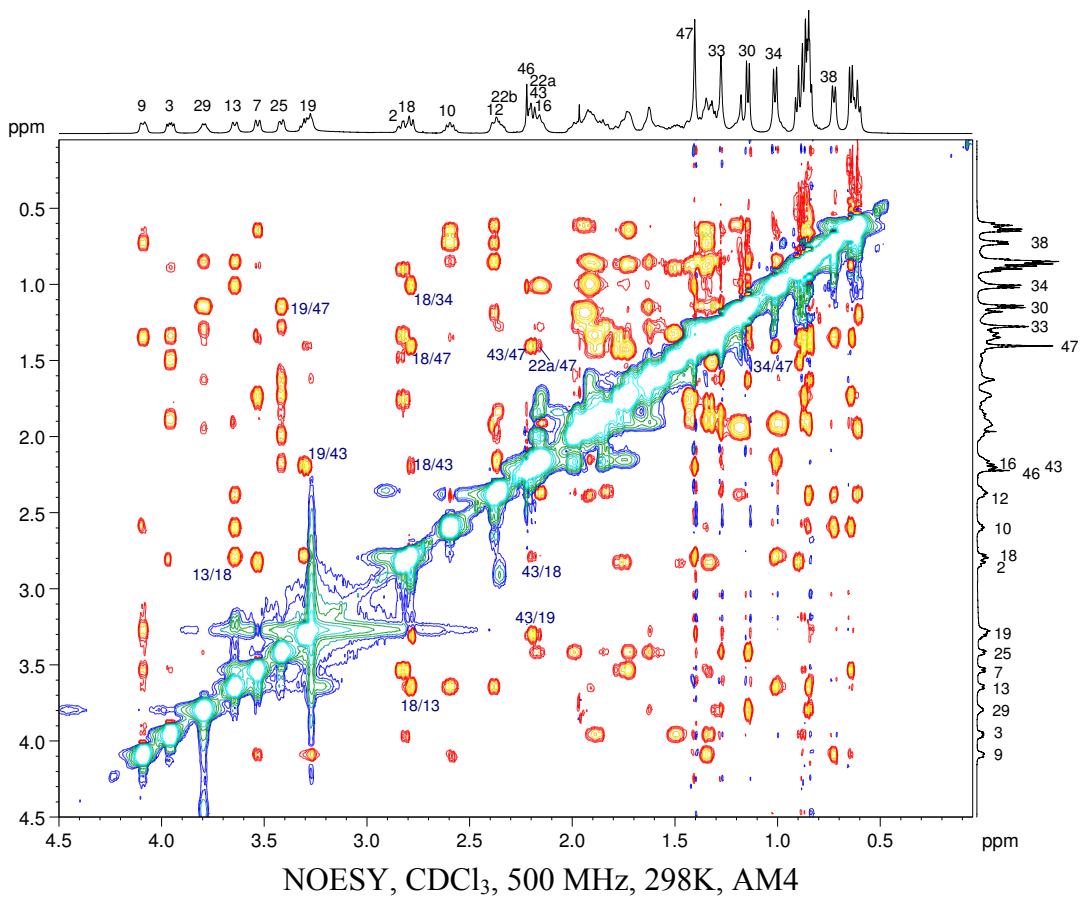
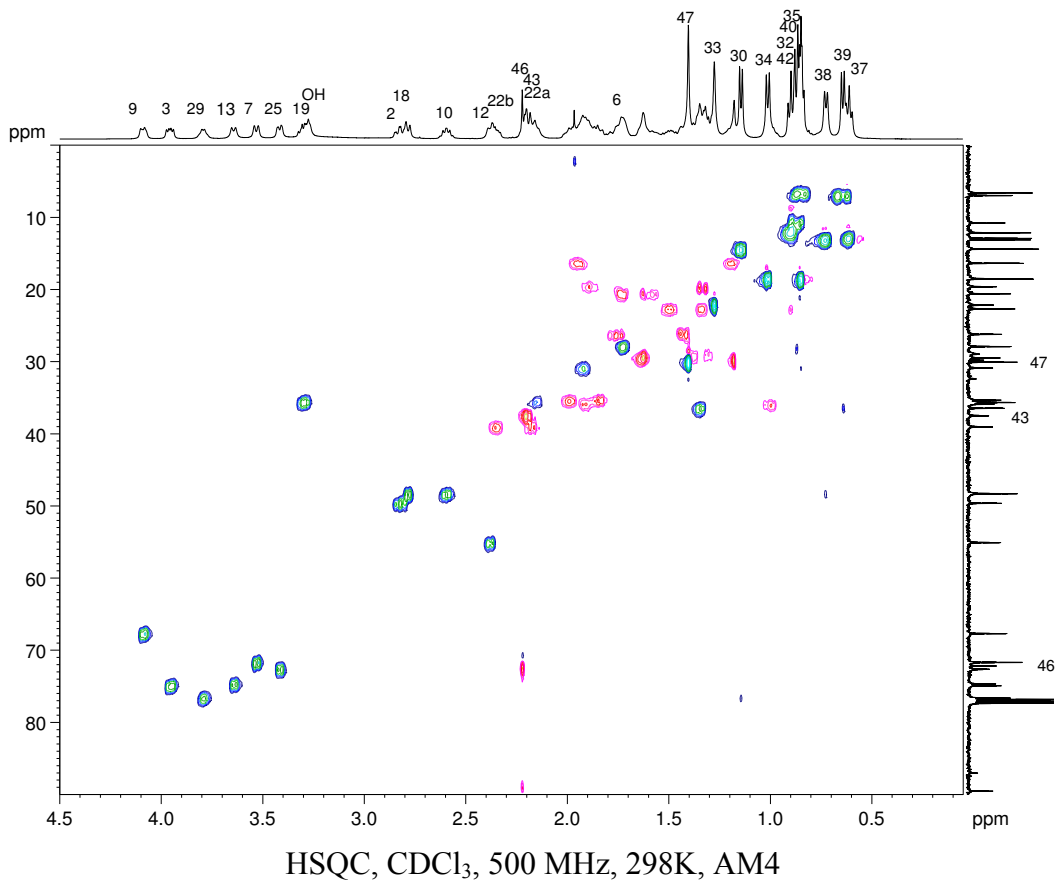


¹H-NMR, CDCl₃, 500 MHz, 298K, AM4



¹³C-NMR, CDCl₃, 500 MHz, 298K, AM4





Material and Methods

Cell culture. Dulbecco's Phosphate-Buffered Saline (14190-094, 500 mL, Gibco), Dulbecco's Modified Eagle Medium (DMEM)/F12 (31331-028, 500 mL, Gibco), DMEM high glucose with UltraGlutamine (BE12-604F/U1, BioWhittaker, Lonza), McCoy's 5A (Modified) Medium (26600-023, Gibco), RPMI 1640 with L-glutamine (BE12-702F/U1, BioWhittaker, Lonza), Fetal Bovine Serum (FBS, 10270-106, Gibco), Hydrocortisone (H0888, Sigma Aldrich), Insulin (I0516 or I9278, Sigma Aldrich), BD Epidermal growth factor human recombinant (hEGF, 354052, BD Biosciences), PEN-STREP (DE17-602E, BioWhittaker, Lonza), Puromycin dihydrochloride (A11138-02, Life Technologies). Human osteosarcoma U2OS cell line (ATCC®, HTB-96™) was cultured in McCoy's 5A or DMEM medium supplemented with 1× PEN-STREP and 10% FBS. MCF-7 (ATCC®, HTB-22™) was maintained in RPMI medium supplemented with 1× PEN-STREP and 10% FBS. The human mammary epithelial cell line infected with a retrovirus carrying hTERT, SV40 and the oncogenic allele *HrasV12*, named HMLER CD44^{high}/CD24^{low} cells, not expressing E-cadherin and expressing Vimentin (referred to as HMLER CD24^{low}) was a generous gift from A. Puisieux (INSERM). HMLER CD24^{low} cells or isogenic non-stem HMLER CD24^{high} cells were cultured in DMEM/F12 supplemented with 10% FBS, 10 µg/mL insulin, 0.5 µg/mL hydrocortisone, 10 ng/mL hEGF, and 0.5 µg/mL puromycin. ICSCL-10A2 cells were cultured in DMEM supplemented with 10% FBS. Primary breast cells were isolated from reduction mammoplasty surgeries performed by V. Mitz (Clinique du Louvre, Paris, France) and were cultured in Epicult™-C medium (Stemcell™ Technologies) supplemented with Epicult™-C and Hydrocortisone. A mycoplasma test was performed using PCR mycoplasma detection kit (G238, Applied Biological Materials).

Cell viability assay. Cell viability assay was carried out by plating 1000 cells/well in 96-well plates. Cells were treated as indicated for 72 h. CellTiter-Blue® reagent (G8081, Promega) was added after 72 h treatment and cells were incubated for 1 h before recording fluorescence intensities (ex. 560/20 nm; em. 590/10 nm) using a Perkin Elmer Wallac 1420 Victor2 Microplate Reader.

Clonogenic assay. HMLER CD24^{low} cells were plated in 6-well plates and incubated with various concentrations of Sal and derivatives for 72 h. Single-cell suspensions were mixed with an equal volume of 0.7% soft agar and plated in 6-well plates (2500 cells/well) for 10 days. After staining with 3-(4,5-dimethyl-2-thiazolyl)-2,5-diphenyl-2H-tetrazolium bromide (MTT, M2128, Sigma Aldrich). Colonies with a diameter of higher than 0.5 mm were counted.

Tumorsphere assay. HMLER CD24^{low} cells were plated as single-cell at 10³ cells/mL in ultra-low attachment culture dishes using a serum-free DMEM/F12 supplemented with B-27 (17504044, Invitrogen, 1:50), 20 ng/mL hEGF, 4 µg/mL insulin and 0.5 µg/mL hydrocortisone. After 7 days, tumorspheres were enzymatically dissociated with 0.05% trypsin (15090, Gibco) for 15 minutes at 37 °C to obtain a single-cell suspension. Sphere formation was assessed 7 days after seeding cells individually in 96-well ultralow attachment plates (Corning), which were treated as indicated. The number and size of tumorspheres were analyzed under a light microscope.

Xenograft tumor formation. MCF-7 cell cultures were collected, enzymatically dissociated, washed with PBS, and re-suspended in a PBS/Matrigel mixture (1:1 v/v). The mixture (0.1 mL) was then implanted in the mammary fat pad of 5-week-old female AthymicNude-Fox1nu

mice bilaterally (Harlan, France). Mice were maintained in individually-ventilated cages (Tecniplast, France) under constant temperature and humidity. All experiments were performed under laminar flow (Tecniplast France). Mice received estradiol supplementation (0.4 mg/kg) the same day and 7 days from cell injection, and were observed and palpated for tumor appearance. Mice were treated with AM5 (1 mg/kg body weight/day) by means of intraperitoneal injections every 5 working days of the week. Tumor growth was measured weekly using calipers. Tumor volume was determined using the standard formula: $L \times W^2 \times 0.52$, where L and W are the longest and shortest diameters, respectively. All animal studies were approved by the Direction des services Vétérinaires, Préfecture de Police, Paris, France (authorization number A75-14-08) and the ethical committee (number 34) of Paris Descartes Université. No randomization was used and experimenters were blinded to drug treatments and tissue analyses.

Patient derived xenografts (PDXs). PDXs were established as previously described²⁴, from tissue samples collected prospectively at the Institut Paoli-Calmettes (IPC). Samples of human origin and associated data were obtained from the IPC/CRCM Tumor Bank that operates under authorization # AC-2007-33 granted by the French Ministry of Higher Education and Research. Before scientific use of samples and data, patients were appropriately informed and asked to consent in writing, in compliance with French and European regulations. The project was approved by the IPC Institutional Review Board. Cells from 2 different patient-derived xenografts (PDX 1 and 2) were transplanted orthotopically into fat pads of 4-week-old female non-obese diabetic/severe combined immunodeficient (NOD/SCID) mice (NOD.CB17-Prkdc^{scid}/J, Charles River France) after mechanical treatment and enzymatic digestion using collagenase/hyaluronidase (StemCell Technologies) to generate single-cell suspension suitable for implantation *in vivo*. PDXs were primarily established as previously described and evaluated for ALDEFLUOR-positive CSCs²⁴. We injected single cancer cells into fat pads of NOD/SCID mice and monitored tumor growth. When tumor size reached approximately 150 mm³, Sal and AM5 treatment were performed as indicated in Fig. 1. Tumor growth was compared with that of docetaxel and placebo-treated controls. After 4 weeks of treatment, the animals were sacrificed and the proportion of ALDEFLUOR-positive CSCs was measured in each residual tumor. All animal studies were approved by the French Ministry of Higher Education and Research (authorization number D130554) and ethical committee (number 14), of Aix-Marseille Université. No randomization was used and experimenters were blinded to drug treatments and tissue analyses.

Aldefluor assay. The analysis was processed on single-cell suspension from the PDXs obtained as described above. The ALDEFLUOR Kit (StemcellTM Technologies) was used to isolate the population with high aldehyde dehydrogenase enzymatic activity using an LSR2 cytometer (Becton Dickinson Biosciences) as previously described²⁴. To eliminate cells of mouse origin from the PDXs, we used staining with an anti-H2Kd antibody (BD Biosciences, 1:200, 20 min on ice) followed by staining with a secondary antibody labeled with phycoerythrin (PE; Jackson Laboratories, 1:250, 20 min on ice).

Limiting dilution assay. Cells from 4-week treated mice were re-implanted into one to four secondary NOD/SCID mice with injection of 10, 50, 500 or 5000 cells for each treated tumor to functionally evaluate the proportion of residual CSCs in each group of treatments (Unt., Doc, Sal, AM5) for the PDX 1 and 2. Each mouse that developed a tumor reaching a size of 10 mm was considered as a tumor-bearing mouse.

Estimation of number of CSCs *in vivo*. The number of mammary gland outgrowths obtained in a fat pad after cell re-implantation is currently used to evaluate the number of stem cells able to repopulate this fat pad. It is based on self-renewal and differentiation abilities, two hallmarks of stem cells. In the same manner, estimation of the number of CSCs can be obtained from tumor outgrowth data collected after limited dilution re-implantation of each group of treatments, based on tumor-initiating capacities of CSCs. For calculation, an online tool is available using Extreme Limiting Dilution Analysis (ELDA) (<http://bioinf.wehi.edu.au/software/elda/>) for limiting dilution analysis based on the Poisson single-hit model according to the number of outgrowths observed and the number of fat pad re-implanted for each cell dilution.

Histology. Organs from mice were removed at time of sacrifice. For morphological analyses, organs were fixed with 4% paraformaldehyde, paraffin embedded, and 4- μ m sections were stained with hematoxylin and eosin (H&E). Sections were scanned at high resolution using a slide scanner (NanoZoomer 2.0-HT, Hamamatsu, Massy, France). Representative images are shown in the main text and Supplementary data.

Immunoblotting. Cells were treated as indicated, then washed twice with PBS and lysed with 2 \times Laemmli buffer. Protein extracts were heated at 95 °C for 5 min, sheared through a 26-gauge needle and quantified with a Nanodrop 2000 (Thermo Fisher Scientific). Protein lysates (~100 μ g) were resolved by SDS-PAGE electrophoresis and transferred onto PVDF membranes (Amersham). Membranes were blocked with 5% BSA, 0.1% Tween-20/TBS for 1 h. The blots were then probed with the relevant primary antibodies in 5% BSA, 0.1% Tween-20/TBS at 4 °C overnight with gentle agitation. Membranes were washed with 0.1% Tween-20/TBS for 30 min and were incubated with secondary antibodies for 1 h at room temperature. Antigens were detected by ECL (Amersham). Imaging was performed using a ChemiDocTM XRS+ System (Biorad).

Intracellular sodium measurements. Sodium and potassium buffers (10 mM HEPES, 1 mM CaCl₂, 1 mM MgCl₂, 130 mM Sodium-D-Gluconate or Potassium-D-Gluconate, 30 mM NaCl/KCl) were mixed at different ratios to produce five buffers with various sodium concentrations (0, 20, 40, 80, 160 mM). Nigericin (N7143, Sigma Aldrich, 10 μ M) and monensin (M5273, Sigma Aldrich, 10 μ M) were used to equilibrate the intracellular sodium concentration and establish a calibration curve. Cells were harvested and re-suspended in ECS buffer (15 mM HEPES, 5.4 mM KCl, 140 mM NaCl, 10 mM Glucose, 1 mM MgCl₂, 1.8 mM CaCl₂, 0.1% BSA, pH 7.6) containing 10 μ M of the sodium-specific probe (SBFI-AM, S-1263, Molecular Probes®) and 0.2% Pluronic F-127 (P2443, Sigma Aldrich) and were incubated for 1 h in the dark at 37 °C. Then, cells were washed to remove excess dye and incubated for an additional 30 min in ECS buffer. Cells were introduced into a 96-well plate (1000 cells/well) and treated as indicated for 1 h prior to fluorescence measurement. Each well was sequentially excited at 340 and 370 nm and emission was recorded at 500 nm. The spectral response of SBFI upon sodium binding was assessed by ratiometric measurements (340/370 nm). Measurements were performed on a Perkin Elmer Wallac 1420 Victor2 Microplate Reader at 37 °C.

Acridine orange (AO) assay. Cells were treated as indicated in the figure prior to treatment with a 2 μ g/mL acridine orange solution for 20 min (37 °C, 5% CO₂), then washed with PBS and immediately observed. Images were obtained using a Leica TCS SP5 confocal microscope equipped with an argon laser (ex. 488 nm), and a Plan-Apochromat 63 \times /1.4 oil objective lens. AO produces red fluorescence (emission peak at about 650 nm) in the

lysosomal compartments and green fluorescence (emission peak between 530 and 550 nm) in the cytosolic and nuclear compartments. ImageJ® was used for further image processing.

Localization of intracellular iron(II). The iron(II) selective fluorogenic probe RhoNox-1 was synthesized according to the original report²⁹. Cells were seeded on μ -Dishes, then treated as indicated in the main figure. Cells were washed with 1 \times Hank's Balanced Salt Solution (HBSS, 14025-092, Life Technologies) three times, then incubated with 5 μ M of RhoNox-1/HBSS for 1 h at 37 °C, 5% CO₂ and washed with HBSS. Co-staining was performed by adding 100 nM lysotracker deep red and Hoechst 33342 (H1399, Sigma Aldrich, final concentration of 1 μ g/mL) in HBSS. Experiments were performed with a 60 \times APO TIRF oil immersion objective of Nipkow Spinning Disk confocal system (live cell imaging) or a Deltavision real-time microscope (Applied Precision) for fixed cells.

Perls' reaction. Tumors from mice were removed at time of sacrifice. Tumors were fixed with 4% PFA and embedded in paraffin. To monitor accumulation of ferric iron, 4- μ m sections were processed for standard Prussian blue staining. Briefly, slides were deparaffinized in xylenes, rehydrated through a graded ethanol series and subjected to a 1:1 potassium ferrocyanide solution (2%)/hydrochloric acid solution (2%) for 20 min. Then, slides were washed with distilled water (5 min). Nuclear fast red solution was used to stain nuclei. Images were acquired by light microscopy using an inverted microscope (Eclipse Ti-S, Nikon) and 10 \times /0.30, 20 \times /0.50 or 40 \times /0.785 plan fluor objectives (Nikon). Images were captured using a super high definition cooled color camera head DS-Ri1 (Nikon) and NIS Elements software (Nikon).

Lysosomal membrane permeabilization assay. Lysosomal membrane permeabilization (LMP) was assessed by monitoring the release of FITC-dextran (FD10S, 10kDa, Sigma Aldrich) from lysosomes. In brief, cells were incubated with 1 mg/mL FITC-dextran for 2 h at 37 °C. Cells were washed, chased with culture medium for 2 h and treated as indicated for 48 h or with CQ (positive control) for 3 h. Cells were then fixed with 2% formaldehyde/PBS, washed with PBS, mounted and acquired with a 60 \times APO TIRF oil immersion objective of Nipkow Spinning Disk confocal system.

Annexin V-FITC/PI assay. Cells were treated as indicated in the figures. After treatment, cell death was quantified using Annexin V-FITC/Propidium Iodide (PI) assay according to the manufacturer's protocol (Annexin V-FITC Apoptosis Detection Kit II, 556570, BD Pharmingen™). Data were analyzed by a LSRFortessa™ flow cytometer (BD Biosciences, San Jose, CA) and processed using Cell Quest software (BD Biosciences) and FlowJo software (FLOWJO, LLC).

Lipid ROS measurements. Cells were treated with Sal or AM5 (0.5 μ M) as indicated. Then, cells were trypsinized and washed with PBS. Subsequently, cells were incubated with Bodipy-C11® (D3861, Thermo Fisher Scientific, 2 μ M) at 37 °C for 60 min. Next, cells were washed twice with PBS. Oxidation of Bodipy-C11 resulted in a shift of the fluorescence emission peak from 590 nm to 510 nm proportional to lipid ROS generation that was analyzed by LSRFortessa™ flow cytometer (BD Biosciences, San Jose, CA). The data were processed using Cell Quest software (BD Biosciences) and FlowJo software (FLOWJO, LLC). For cell imaging, cells were treated as indicated in the main figure (Bodipy-C11®, 1 μ M, 1 h), then fixed with formaldehyde (2% in PBS, 12 min) and analyzed by fluorescence microscopy (ex. 488 nm).

Intracellular GSH levels quantification. Cells were treated with Sal or AM5 (0.5 μM) as indicated, then harvested and counted. The intracellular GSH level was measured using a commercial kit (ab205811, Abcam) according to the manufacturer's protocol.

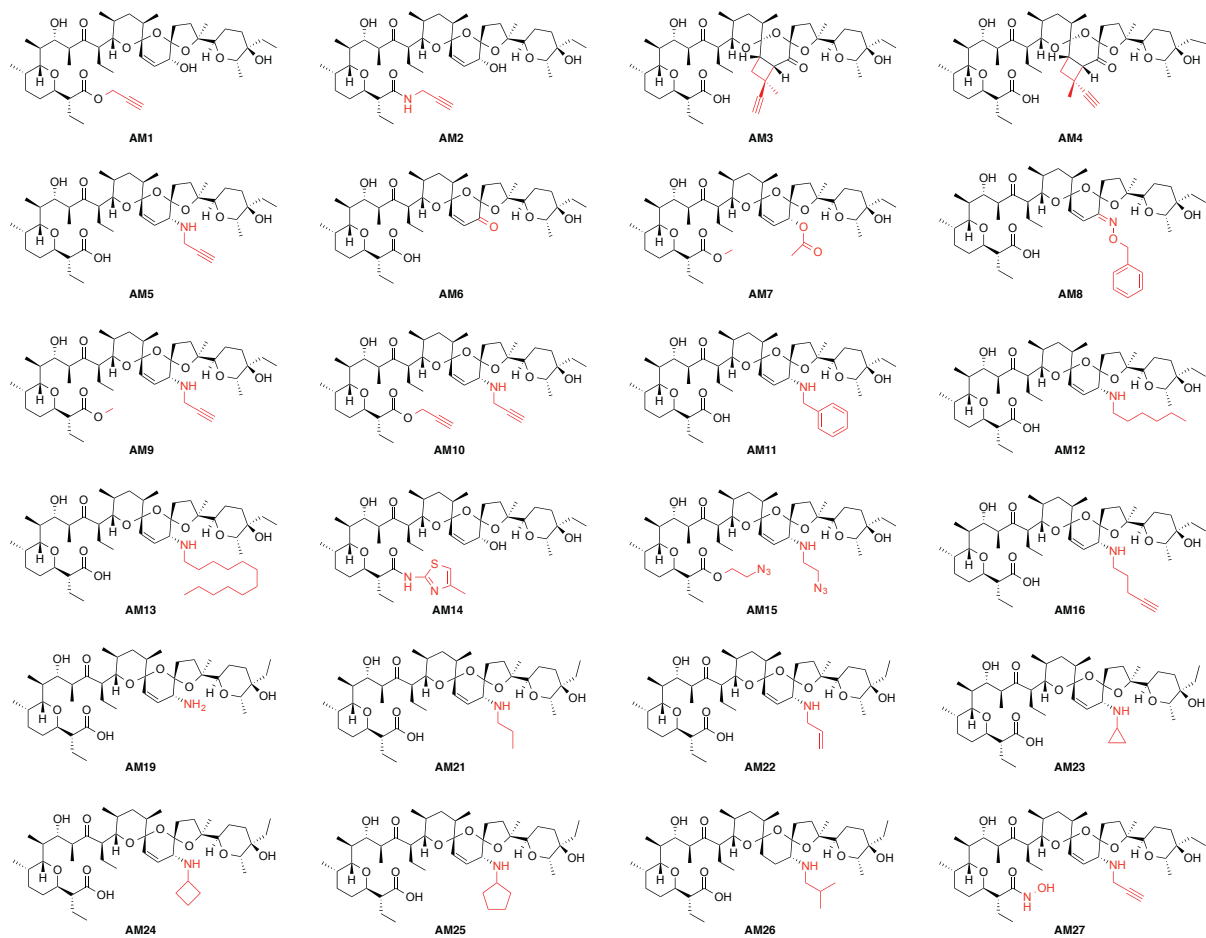
RhoNox-1 reduction assay. Experiments were carried in 96-well plate dishes. Reagent stock solutions were freshly prepared using Milli-Q water. 50 μL of solutions of Sal (800 μM), DFO (800 μM) and FeSO_4 (80 μM) were mixed prior to addition of 50 μL of RhoNox-1 (40 μM) and completed with the appropriate volume of water to reach a final volume of 200 μL per well. Measurements were performed 30 min after addition of RhoNox-1 to the mix and were recorded using the PARADIGM™ Microplate Detection Platform (ex. 492 nm; em. 580 nm).

Electrothermal atomic absorption spectrometry. Cells were harvested, the supernatant was removed, cell pellets were dried and mineralized by adding 100 μL of concentrated nitric acid (PlasmaPure® 67-69% HNO_3 , SCP Science, Baie-d'Urfé, Canada) at 80 °C and further diluted with 400 μL of ultrapure water (Milli-Q®, Millipore, Molsheim, France). Iron was determined in cell mineralisates by means of electrothermal atomic absorption spectrometry (ETAAS) on a PinAAcle® 900Z spectrometer (Perkin Elmer, Les Ulis, France).

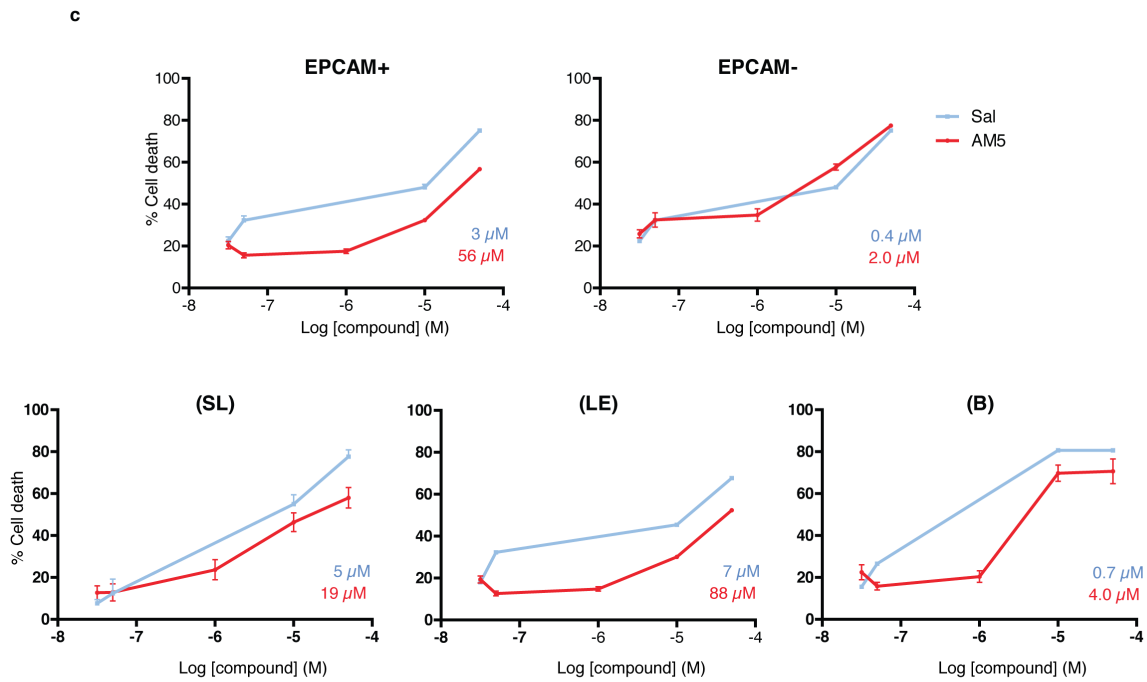
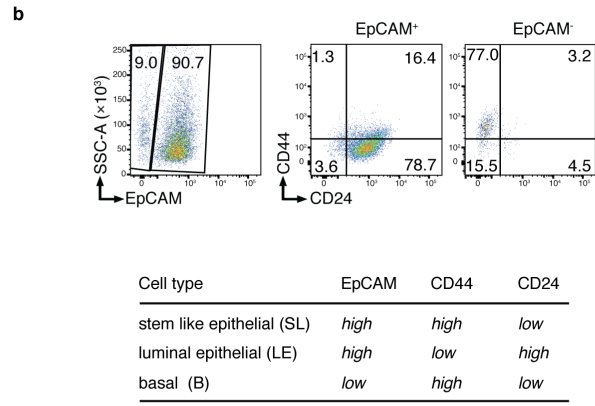
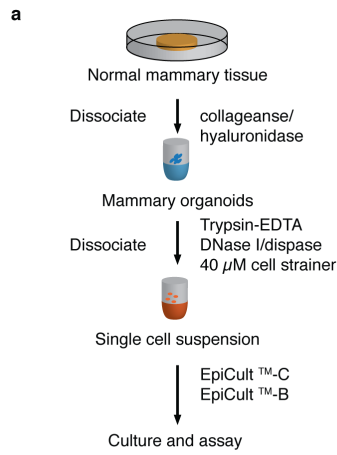
Small interfering RNA transfection. Suitable small interfering RNAs (siRNA) were designed with the Qiagen RNA interference designer tool for specific down-regulation of FTH1. The sequence used for FTH1 was 5'-GUCCAUGUCUUACUACUUUTT-3' (SI00300251) targeting the sequence following 5'-CTGTCCATGTCTTACTACTTT-3' and a negative control siRNA for FTH1 (5'-CAUUAGUUUGGGCAGUAUATT-3', SI03089212). Subconfluent cells were transfected with siRNA in Opti-MEM using the Oligofectamine™ reagent (Invitrogen) for 48 h. Then, cells were treated with OSM (100 ng/mL for 48 h) prior to protein or ARN extraction and flow cytometry analysis for markers as indicated.

RNA extraction and analysis. Total RNA was extracted from tumor cell lines using the NucleoSpin® RNA kit (Macherey-Nagel, Hoerd), according to the manufacturer's protocol. The cDNA was generated from the total RNAs isolated above using oligo(dT) and random hexamer primers, and the M-MLV reverse transcriptase according to the manufacturer's protocol (Invitrogen). Ferritin, snail, zeb1, slug and ERS1 mRNA expression levels were quantified by RT-PCR using iTaq™ Universal SYBR® Green supermix according to the manufacturer's protocol (Bio-Rad) in a CFX96 thermal cycler (Bio-Rad). The data were normalized to the internal control β -actin. Relative gene expression levels were calculated using the delta Ct ($2^{-\Delta\Delta\text{Ct}}$) method. Sequences of the primers used for RT-PCR are: ERS1 (Forward: 5'-AAGCTTCGATGATGGGCTTA-3'; Reverse: 5'-AGGTGGACCTGATCATGGAG-3'), FTH1 (Forward: 5'-CTGGAGCTCTACGCCTCCTA-3'; Reverse: 5'-TCTCAGCATGTTCCCTCTCC-3'), SLUG (Forward: 5'-ACACATTAGAACTCACACGGG-3'; Reverse: 5'-TGGAGAAGGTTTTGGAGCAG-3'), SNAIL (Forward: 5'-GGAAGCCTAACTACAGCGAG-3'; Reverse: 5'-CAGAGTCCCAGATGAGCATTG-3'), ZEB1 (Forward: 5'-ACCCTTGAAAGTGATCCAGC-3'; Reverse: 5'-CATTCCATTTTCTGTCTTCCGC-3').

Statistical analysis. Data were compared using a two-tailed Student's *t*-test, a Mann-Whitney *U* test or a one-way ANOVA as indicated. Data are presented as mean values. Two groups were considered to be significantly different if $P < 0.05$.



Supplementary Figure 1 | Molecular structures of synthetic derivatives of Sal.

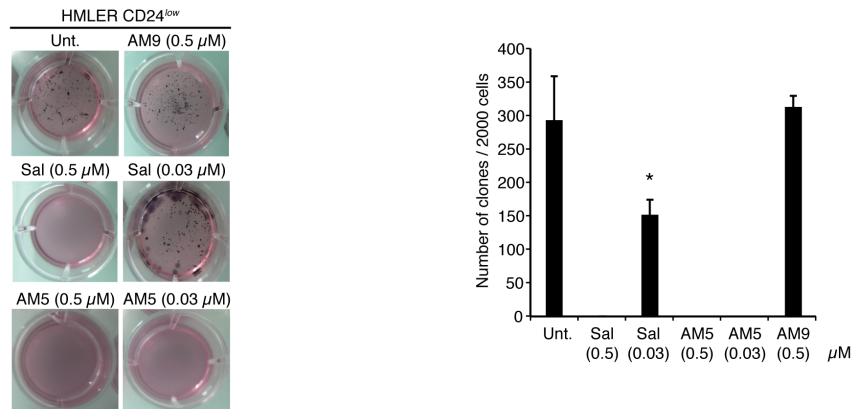


d

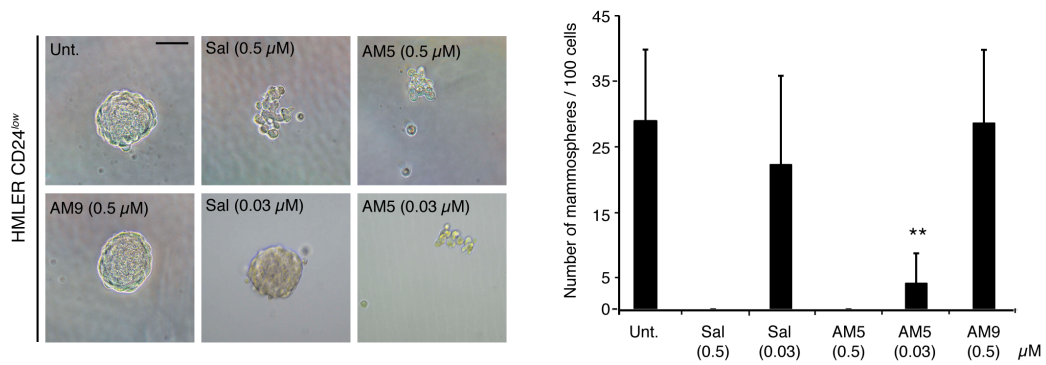
	Cell type	Cell subtype	IC ₅₀	
			Sal [μM]	AM5 [μM]
Breast primary cells	Normal	EpCAM ⁺	3	56
		(SL)	5	19
		(LE)	7	88
		EpCAM ⁻	0.4	2
		(B)	0.7	4
Breast cell lines	Normal	MCF-10A	>1	>1
	CSCs	iCSC-10A2	0.3	0.02

Supplementary Figure 2 | Sal and AM5 selectively target breast CSCs over primary breast cells. a, Schematic illustration of a method for isolating primary breast cells. **b,** Flow cytometry analyses of primary breast cells based on differentiation markers including EpCAM (Epithelial Cell Adhesion Molecule), CD44 and CD24. **c,** Quantification of cell death in cells treated with Sal (blue lines) or AM5 (red lines) for 96 h measured by flow cytometry using DAPI staining. Bars and error bars, mean values and s.d. of a biological triplicate. **d,** Comparative IC₅₀ values of Sal and AM5 against a panel of primary breast cells, a normal breast cell line and a cancer stem cell line.

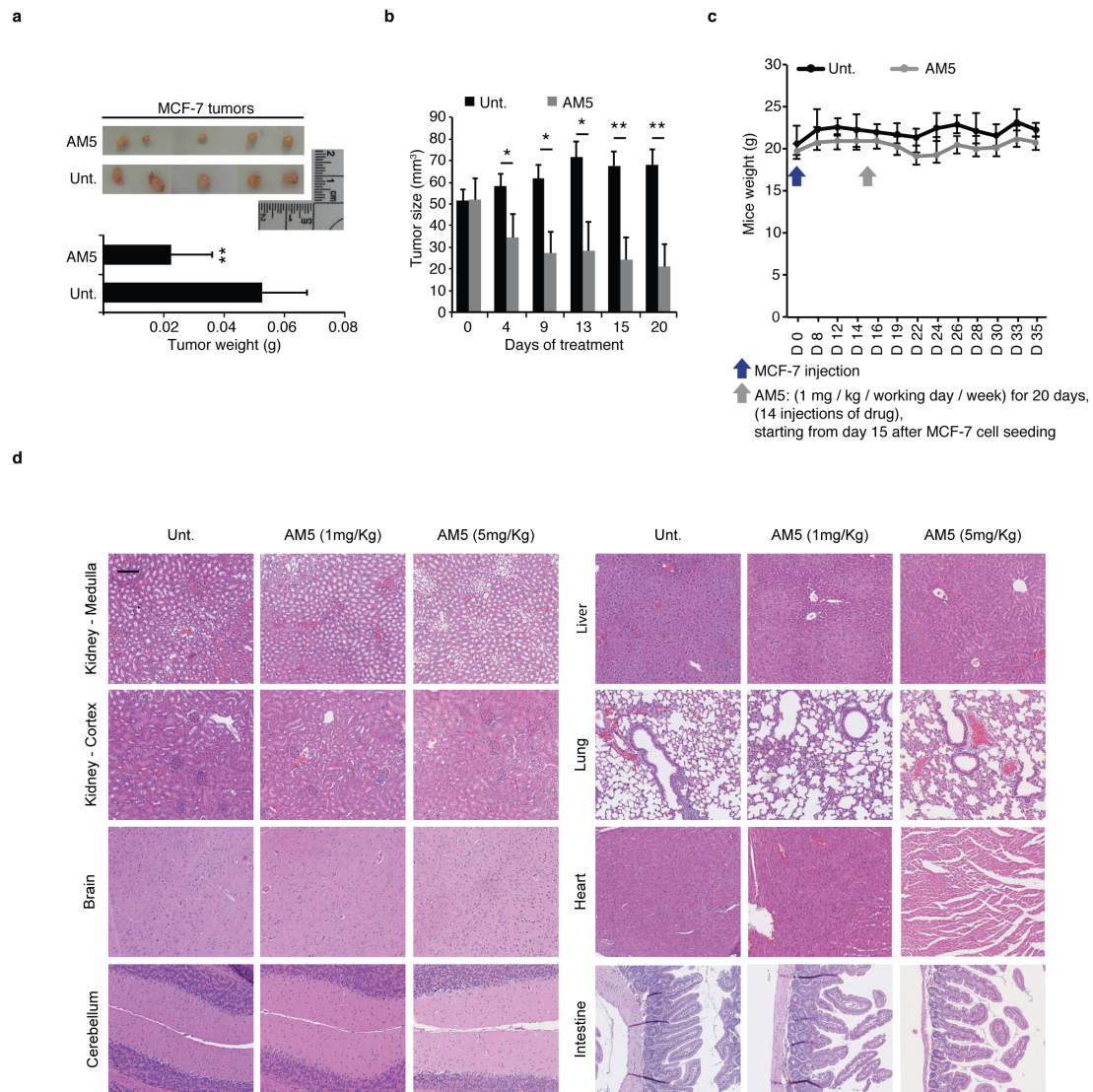
a



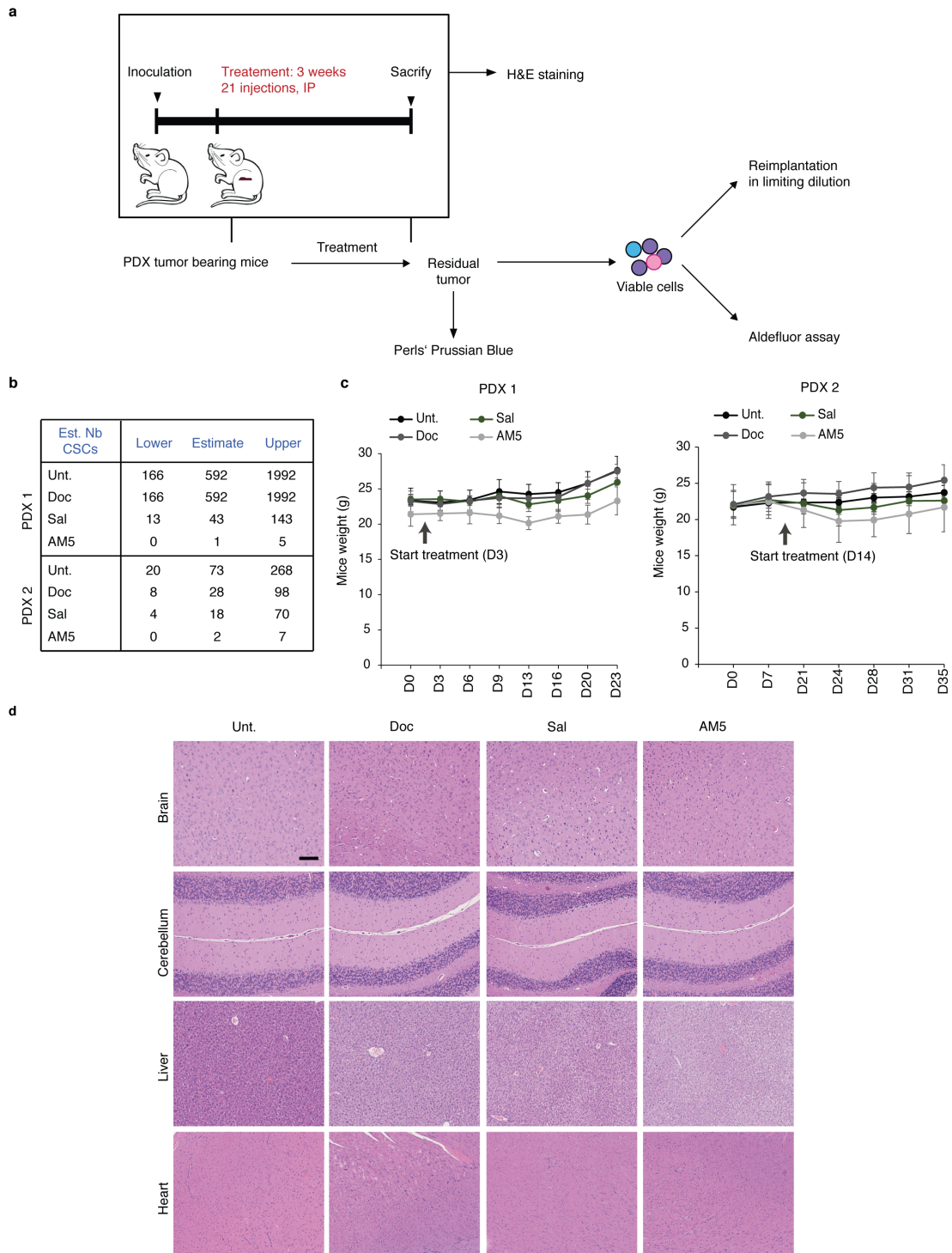
b



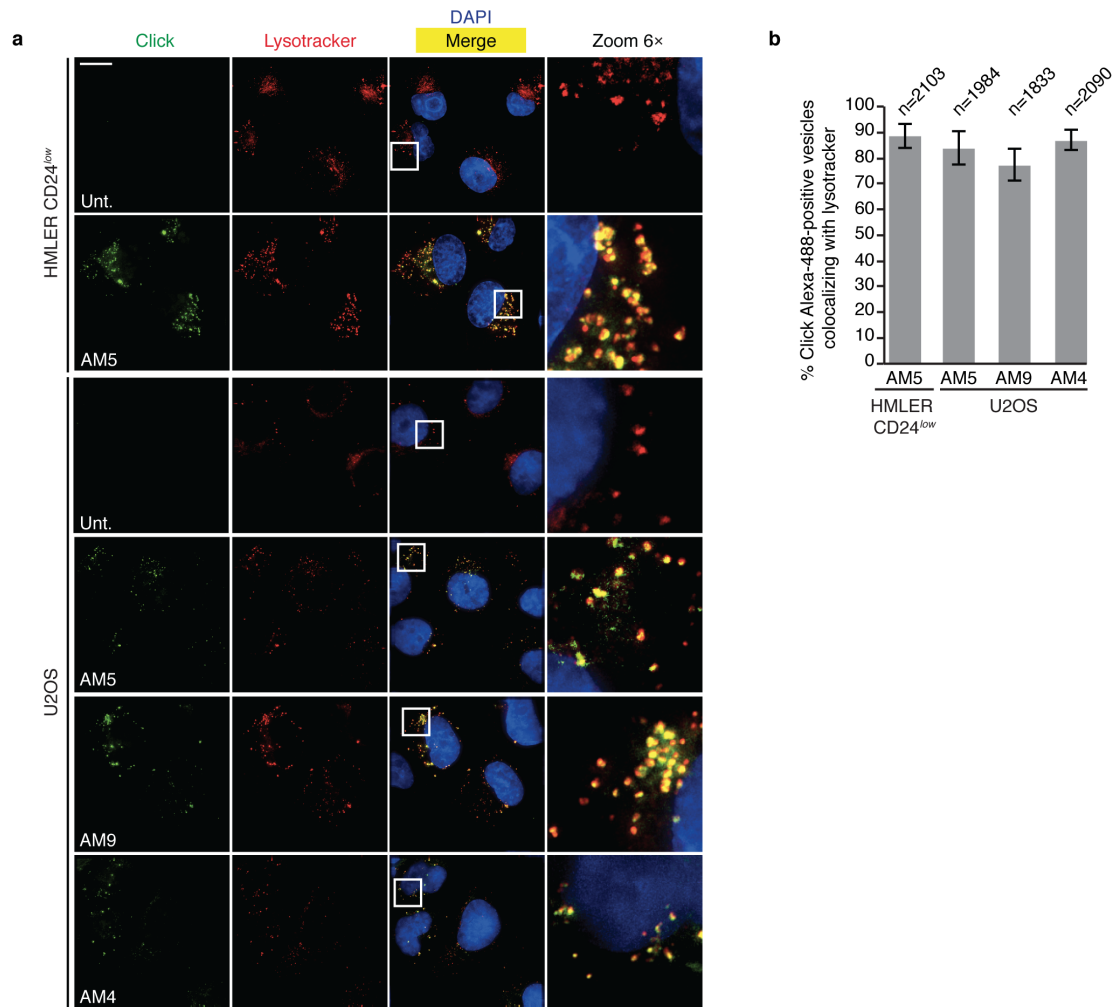
Supplementary Figure 3 | AM5 targets CSCs *in vitro*. **a**, Images of colonies developed from individual HMLER CD24^{low} cells 10 days after being treated as indicated for 72 h. Bars and error bars, mean values and s.d. of three technical replicates. * $P < 0.05$, Student's *t*-test. **b**, Images of secondary tumorspheres formed from individual HMLER CD24^{low} cells 7 days after treatment as indicated. Bars and error bars, mean values and s.d. of three biological replicates. ** $P < 0.01$, Student's *t*-test. Scale bar, 100 μm.



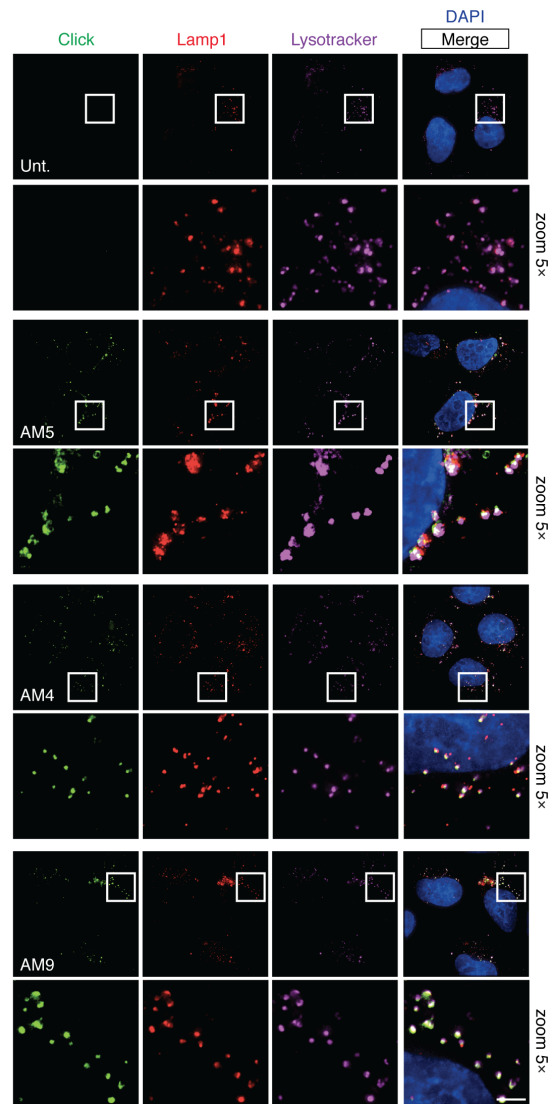
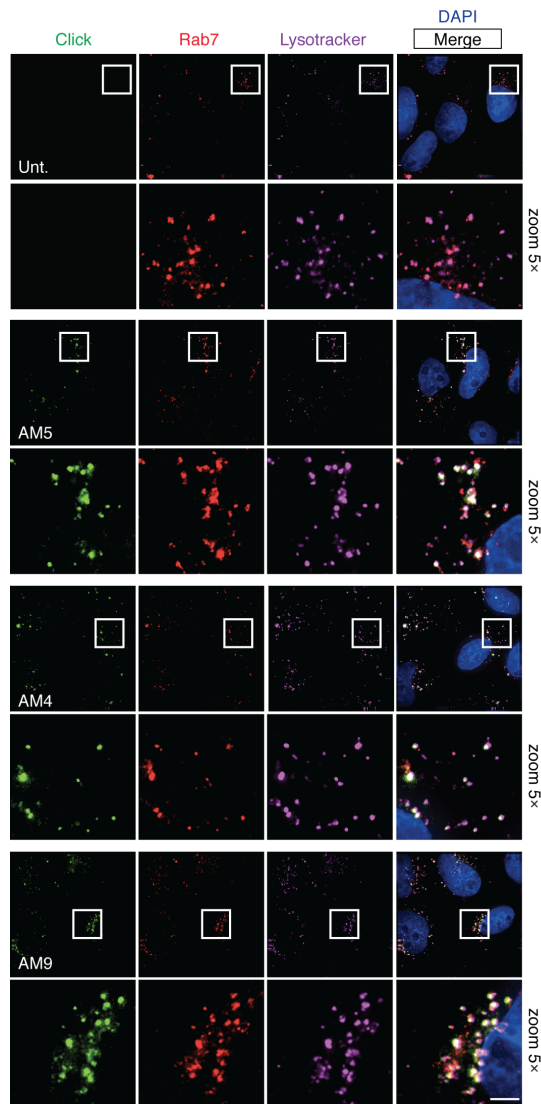
Supplementary Figure 4 | AM5 reduces MCF-7 tumor growth. a, *In vivo* antitumor effect of AM5 in MCF-7 tumor-bearing nude mice treated as indicated for two weeks with vehicle and AM5 (1 mg/kg/day) by means of intraperitoneal injections. Bars and error bars for tumor weight, mean values and s.d. (n=10). ** $P < 0.01$, Student's *t*-test. Bars and error bars for tumor size represent the mean values and s.d. (n=10). * $P < 0.05$, ** $P < 0.01$, Mann-Whitney *U* test. **b,** Quantification of MCF-7 tumor size treated as in **a**. **c,** Evolution of mice body-weight during treatment with AM5. Data points and error bars for mice body weight, mean values and s.d. (n=5 per group). **d,** Comparative hematoxylin and eosin staining images of peripheral tissues of mice treated as in **a**, data representative of five biological replicates. Scale bar, 100 μ m.



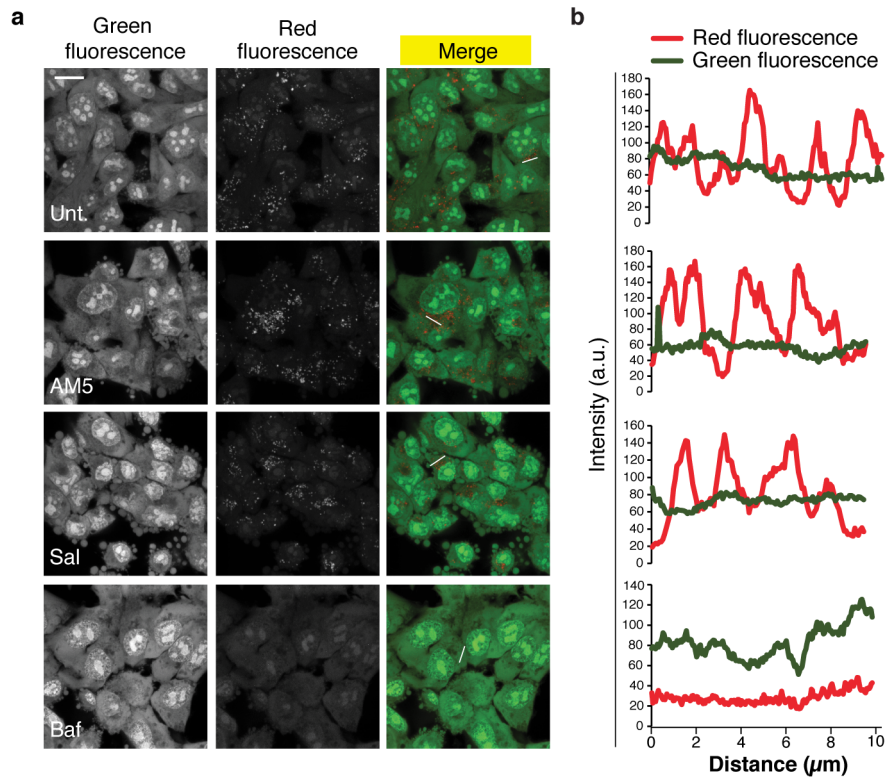
Supplementary Figure 5 | AM5 targets CSCs *in vivo* at non-toxic doses. **a**, Schematic illustration of the methodology employed to monitor CSCs and iron pathway targeting *in vivo*. **b**, Confidence intervals of estimated number of CSCs/10000 cells calculated as in Fig. 1g. **c**, Evolution of mice body-weight during treatment with AM5. Data points and error bars for mice body weight, mean values and s.d. (n=3 per group). **d**, Comparative hematoxylin and eosin staining images of peripheral tissues of mice treated as in Fig. 1e. Data representative of three biological replicates. Scale bar, 20 μ m.



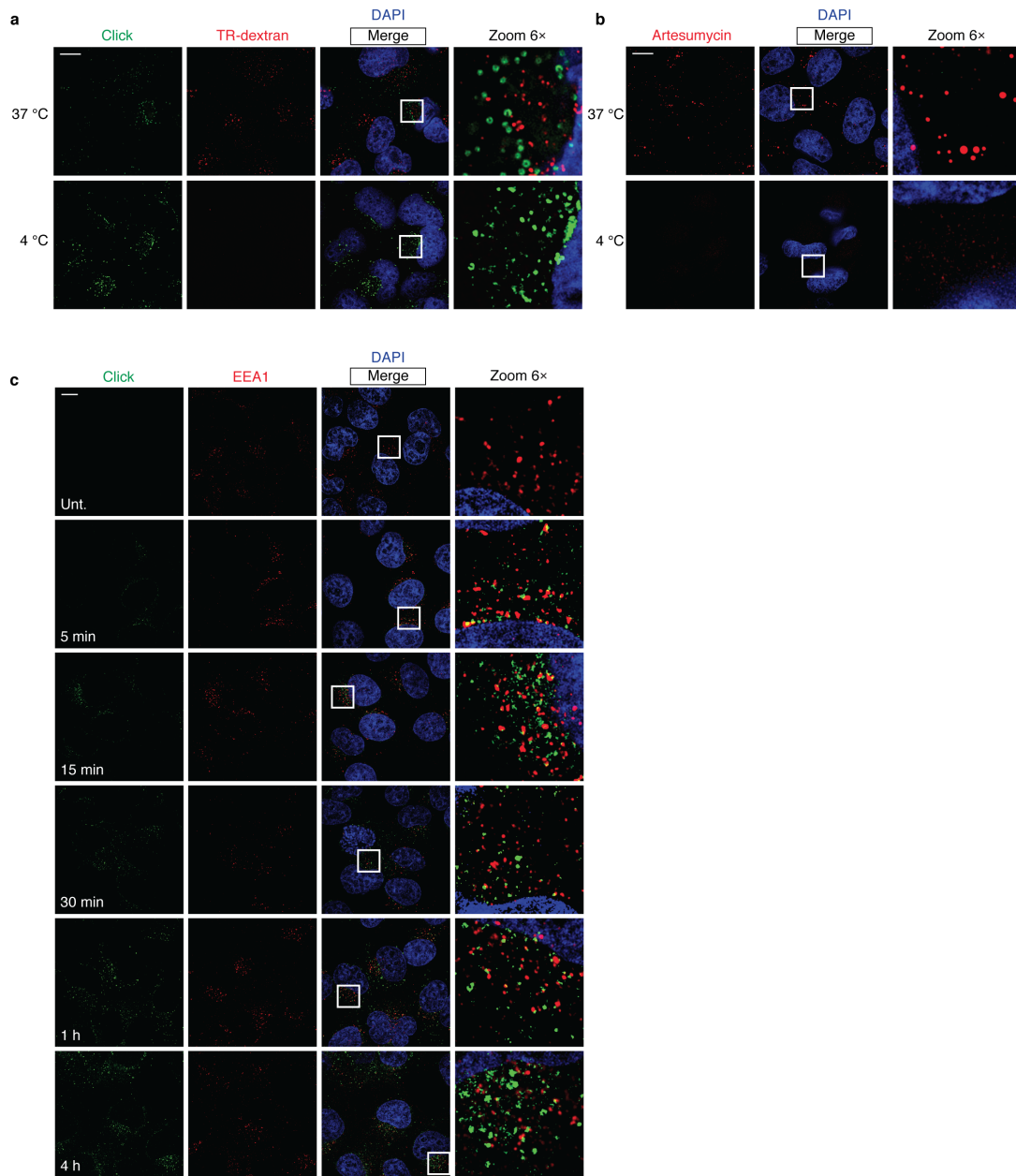
Supplementary Figure 6 | Salinomycin derivatives accumulate quantitatively in lysosomes. a, Fluorescence microscopy images showing the subcellular localization of labeled Sal derivatives in cells treated as indicated (10 μ M, 6 h). Lysotracker deep red stains the lysosomes and 4',6-diamidino-2-phenylindole (DAPI) stains nuclear DNA. Scale bar, 10 μ m. Sal derivatives were labeled by means of click chemistry as described in Methods. **b,** Quantification of click Alexa-488-positive vesicles with lysotracker deep red was carried out by means of visual inspection. At least 90 cells were counted per condition. Data represent three independent biological replicates (n=number of click Alexa-488-positive vesicles). Bars and error bars, mean values and s.d. of three biological replicates.



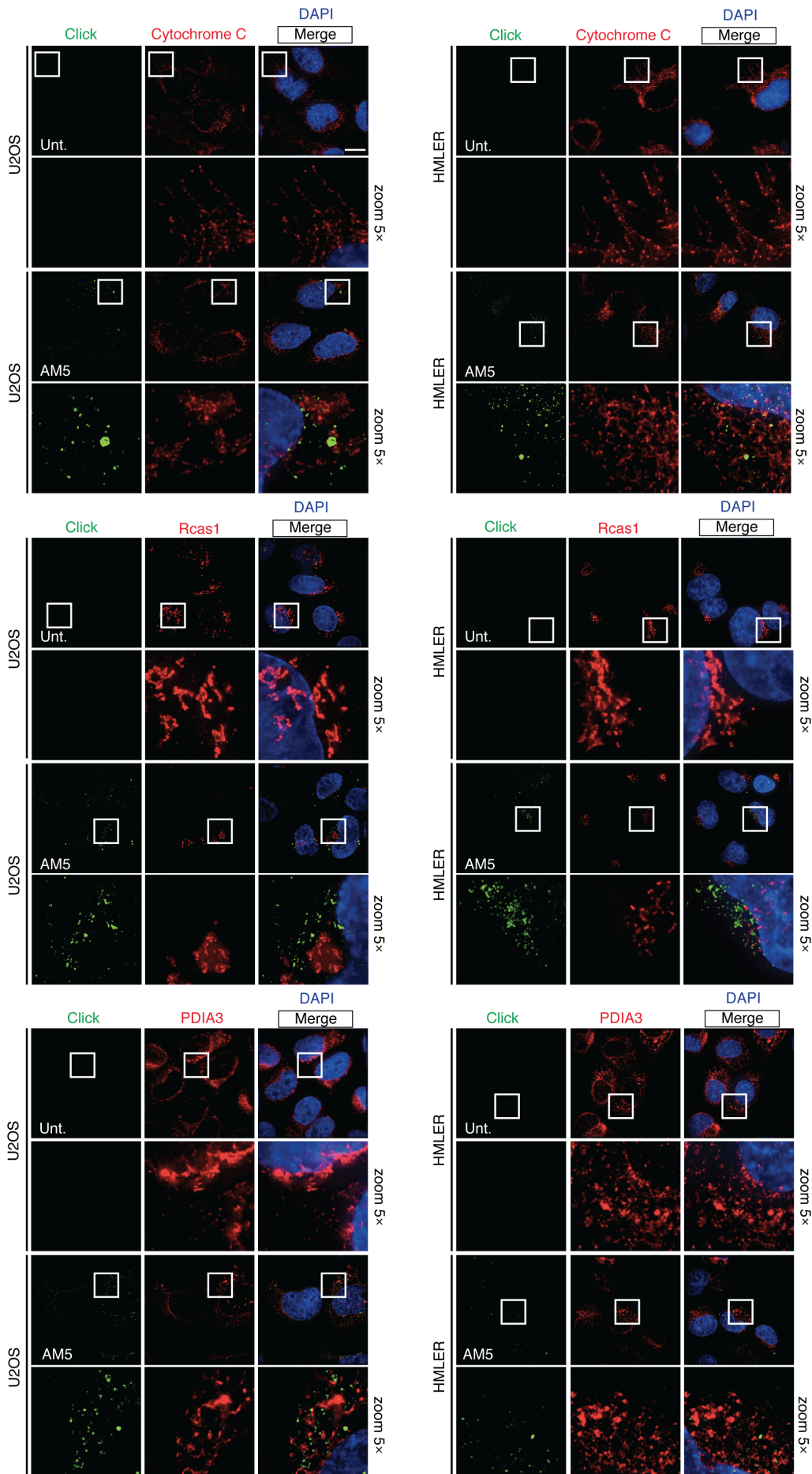
Supplementary Figure 7 | Sal derivatives colocalize with the lysosomal markers Rab7 and Lamp1. Fluorescence microscopy images showing the subcellular localization of labeled Sal derivatives in U2OS cells treated as indicated (10 μ M, 6 h). Rab7 and Lamp1 stain lysosomes and 4',6-diamidino-2-phenylindole (DAPI) stains nuclear DNA. Scale bars, 10 μ m.



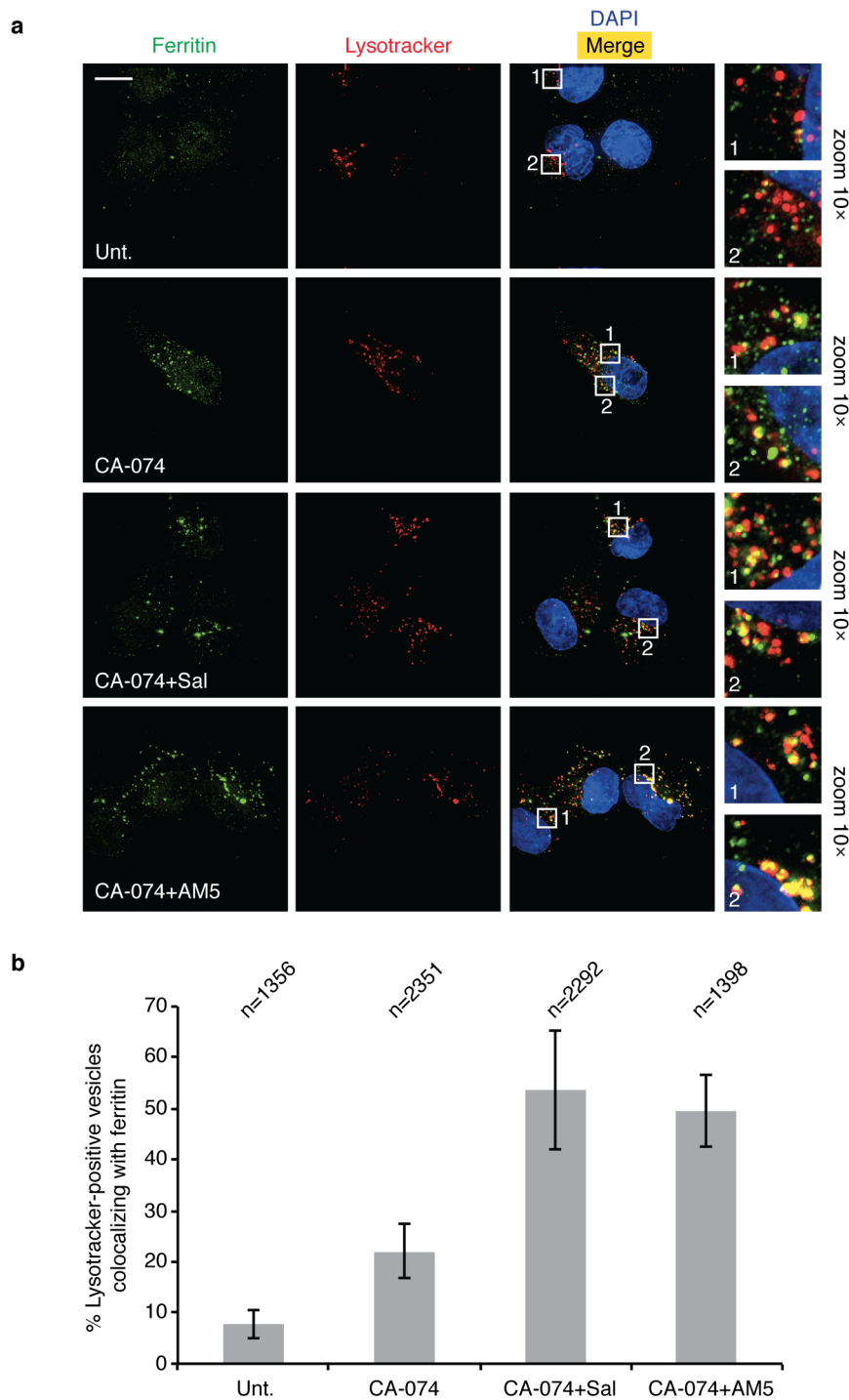
Supplementary Figure 8 | Sal and AM5 do not alter the lysosomal pH. **a**, Fluorescence microscopy images of HMLER CD24^{low} cells treated with Sal or AM5 (0.5 μM) for 16 h prior to incubation with acridine orange (AO). Increase lysosomal pH can be detected by loss of AO fluorescence at 650 nm. Scale bar, 15 μm . **b**, Maximum fluorescence intensity profile line tracings of both fluorescent channels established using the Plot Profile function in ImageJ®. Baf, Bafilomycin A1.



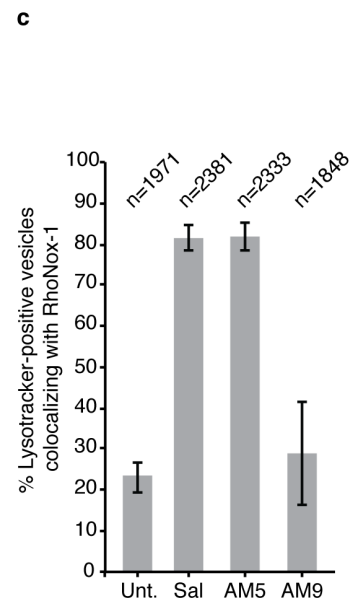
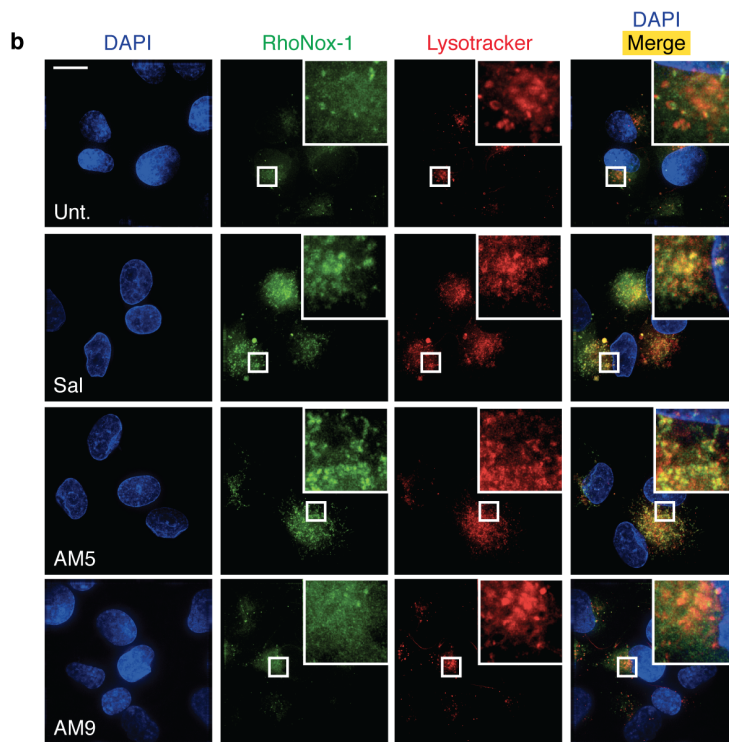
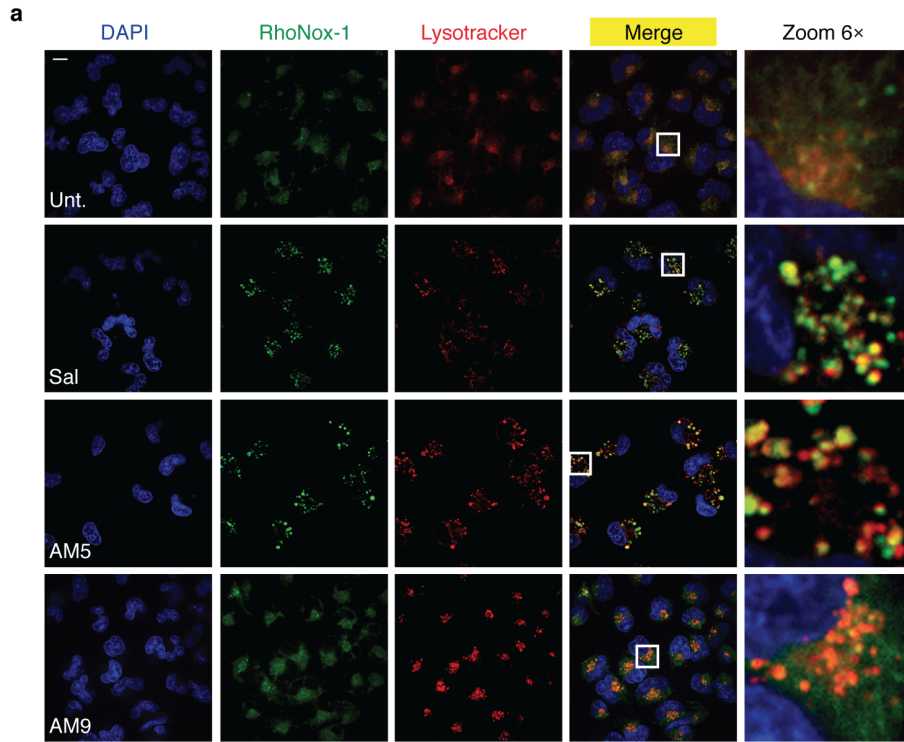
Supplementary Figure 9 | AM5 enters cells independently of endocytosis. **a** and **b**, Fluorescence microscopy images of HMLER CD24^{low} cells showing the subcellular localization of labeled AM5 (green), TR-dextran (red), artesumycin (ex. 555 nm; em. 605 nm) and DAPI (blue). Cells were co-incubated with AM5 (10 μM, 30 min) and TR-dextran (1 mg/mL, 30 min) or with artesumycin (10 μM, 30 min) at the indicated temperature. **c**, Fluorescence microscopy images of HMLER CD24^{low} cells showing the subcellular localization of labeled AM5 (green) and the endosomal marker EEA1 (red). Cells were treated with AM5 (10 μM) for the indicated times at 37 °C. AM5 was labeled by means of click chemistry as described in Methods. Scale bars, 10 μm.



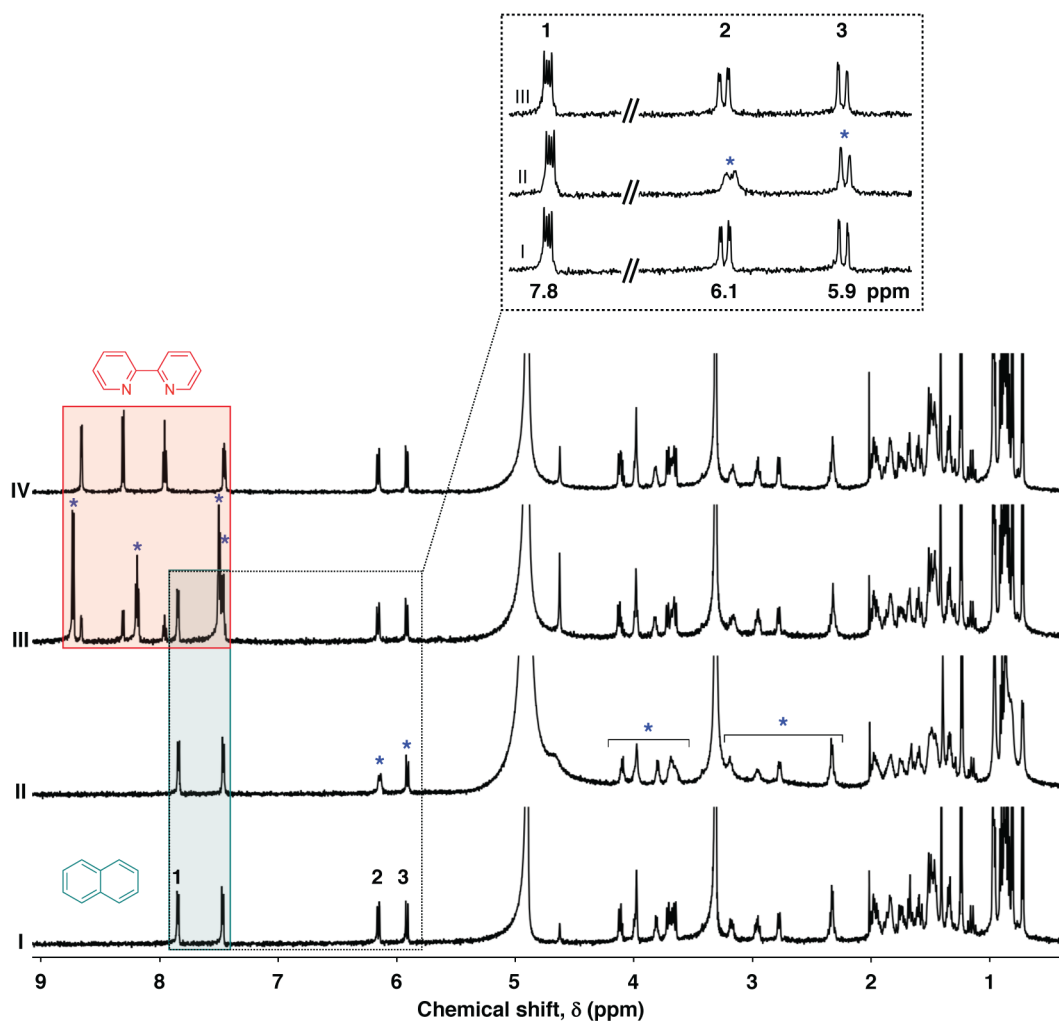
Supplementary Figure 10 | Labeled AM5 does not colocalize with markers of the ER, mitochondria or Golgi. Fluorescence microscopy images of cells showing the subcellular localization of labeled AM5 (green). Cells were treated with AM5 (10 μ M) for 6 h. The endoplasmic reticulum, mitochondria and Golgi apparatus were detected using antibodies against PDIA3, Cytochrome C and Rcas1, respectively. AM5 was labeled by means of click chemistry as described in Methods. Scale bar, 10 μ m.



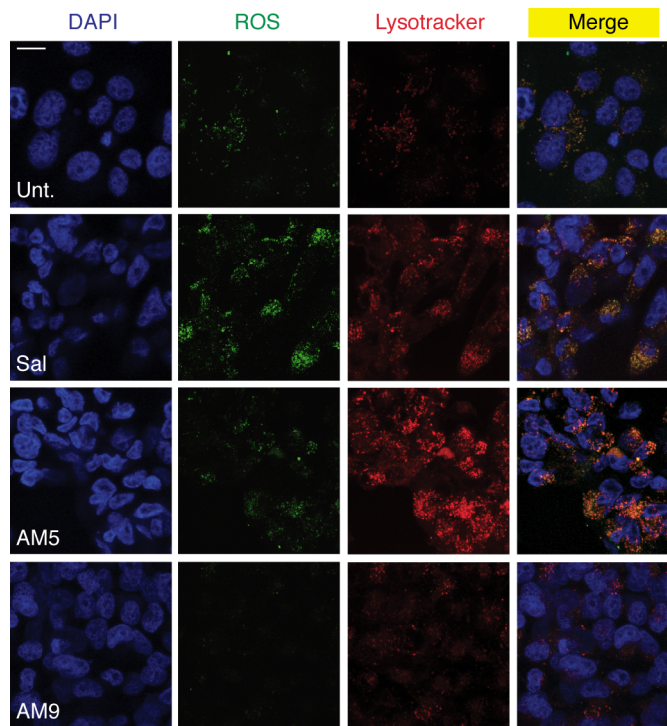
Supplementary Figure 11 | Ferritin co-localizes with lysotracker in cells treated with Sal or AM5. a, Fluorescence microscopy images of HMLER CD24^{low} cells treated with Sal or AM5 (0.5 μ M) in the presence of CA-074 for 6 h, showing the localization of ferritin (green) and lysotracker (red). Lysotracker deep red stains the lysosomes and DAPI stains nuclear DNA (blue). Scale bar, 10 μ m. **b,** Quantification of lysotracker-positive vesicles colocalizing with ferritin was carried out by means of visual inspection. At least 60 cells were counted per condition. Data represent three independent biological replicates (n=number of lysotracker vesicles). Bars and error bars, mean values and s.d. of three biological replicates.



Supplementary Figure 12 | Sal and AM5 sequester iron in lysosomes. **a**, Live cell fluorescence microscopy images showing the subcellular localization of iron(II) using the fluorogenic reduction of RhoNox-1 (green) in HMLER CD24^{low} cells treated with Sal or AM5 (0.5 μ M) for 48 h. Lysotracker deep red stains the lysosomes (red) and DAPI stains nuclear DNA (blue). Scale bar, 10 μ m. **b**, Fixed cell fluorescence microscopy images showing the subcellular localization of iron(II) using the fluorogenic reduction of RhoNox-1 (green) in HMLER CD24^{low} cells treated with Sal or AM5 (0.5 μ M) for 48 h. **c**, Quantification of lysotracker-positive vesicles colocalizing with RhoNox-1 in fixed cells was carried out by means of visual inspection. At least 75 cells were counted per condition. Data represent three independent biological replicates (n=number of lysotracker vesicles). Bars and error bars, mean values and s.d. of three biological replicates.

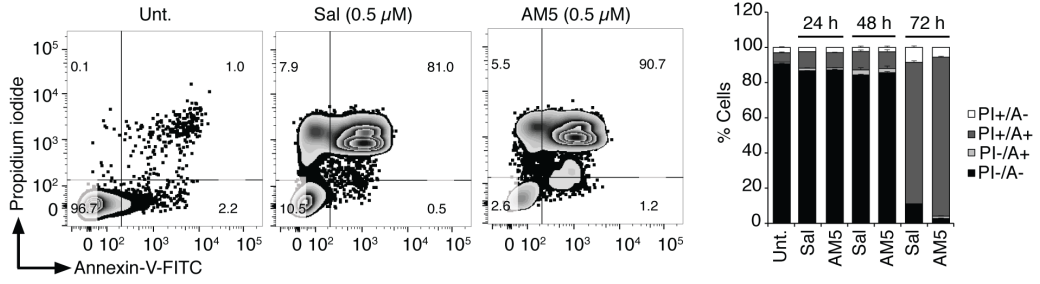


Supplementary Figure 13 | Sal interacts with iron(II) in solution. ¹H-NMR spectra of I. Sal (2 mM) and Napht (1.0 mol equiv.), II. Sal and Napht, in the presence of FeCl₂ (0.5 mol equiv.), III. Sal, Napht and Bipy (1.6 mol equiv.) in the presence of FeCl₂ (Bipy added after FeCl₂), IV. Sal and Bipy. Samples prepared in CD₃OD, spectra recorded at 298 K, 5 min following sample preparation (600 MHz). Blue stars indicate proton signals shielded by iron(II), green and red boxes highlight signals of free Napht and free/bound Bipy, respectively.

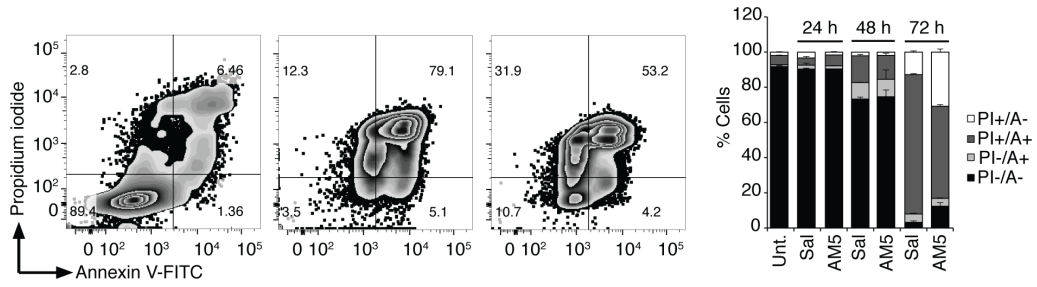


Supplementary Figure 14 | Sal and AM5 induce the production of ROS in HMLER CD24^{low} cells. Fluorescence microscopy images showing the subcellular localization of ROS (green) by means of fluorogenic reaction with CM-H2DCFDA in cells treated as in Fig. 3a. Lysotracker deep red stains the lysosomes (red) and DAPI stains nuclear DNA (blue). Scale bar, 10 μ m.

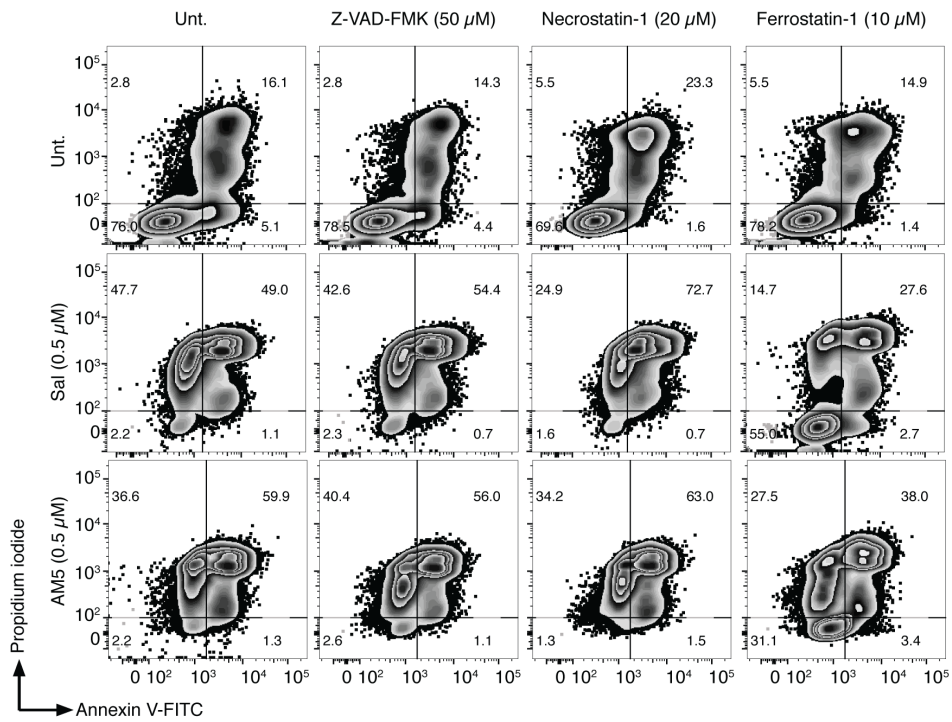
a HMLER CD24^{low}, 72 h



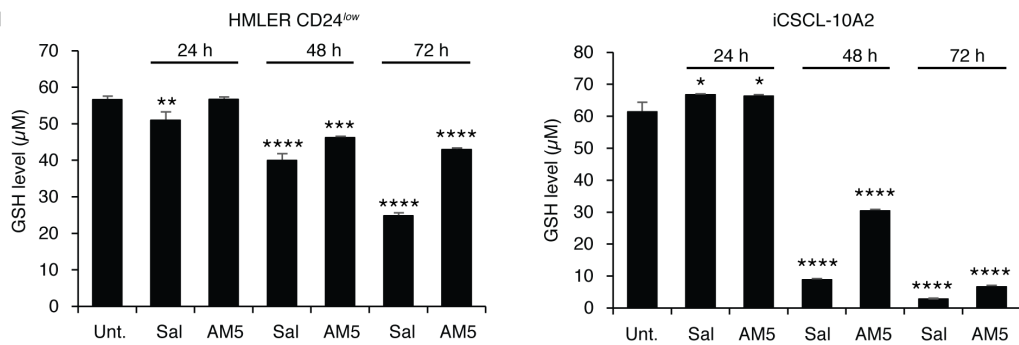
b iCSCL-10A2, 72 h



c iCSCL-10A2, 72 h

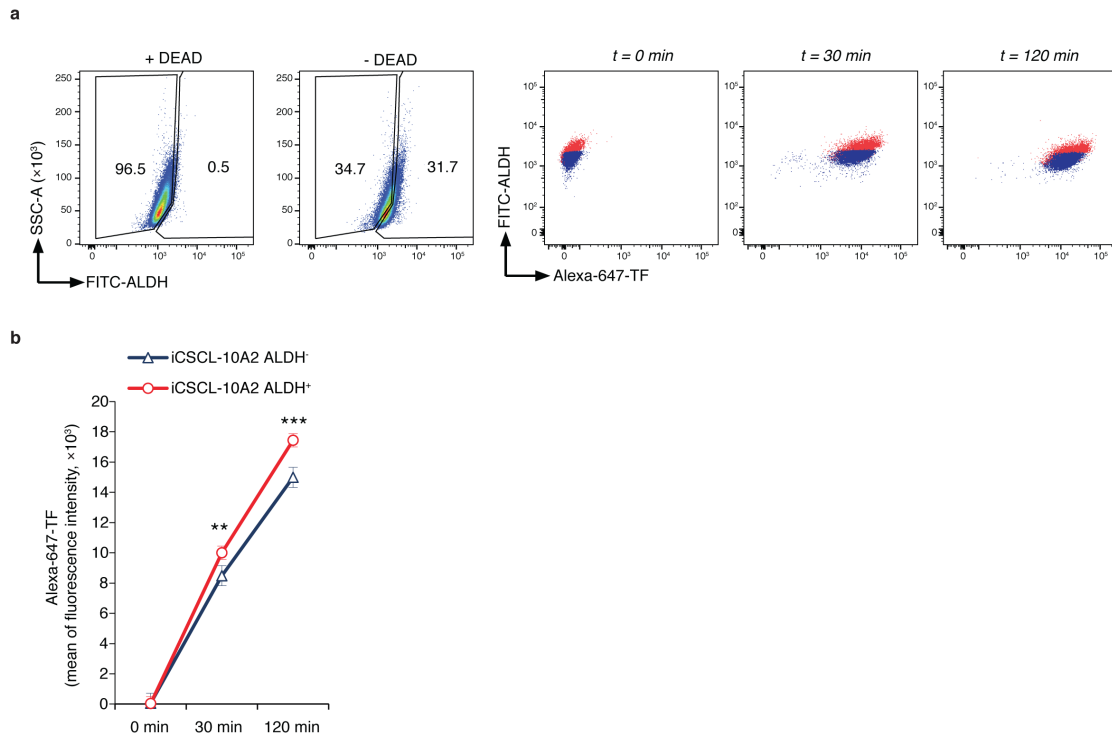


d



Supplementary Figure 15 | Sal and AM5 induce biochemical features characteristic of ferroptosis. Flow cytometry analysis of Annexin V-FITC (A) and Propidium Iodide (PI) fluorescence in **a**, HMLER CD24^{low} and **b**, iCSCL-10A2 cells treated with Sal (0.5 μ M) or AM5 (0.5 μ M) for 24, 48 or 72 h. **c**, Primary data of the quantification provided in Fig. 3g. **d**, Endogenous levels of GSH in cells treated as indicated, measured as described in Methods. Bars and error bars, mean values and s.d. of two biological replicates. * P <0.05, ** P <0.01, *** P <0.001, **** P <0.0001, one-way ANOVA.

Supplementary Figure 16 | Cell death can be rescued by cathepsin B inhibition, ROS scavenging and iron chelation. **a, b** and **c**, Quantification of cell viability measured by flow cytometry using Annexin V-FITC and PI fluorescence in cells treated with Sal or AM5 (0.5 μ M) for 72 h +/- CA-074, NAC or Asc as described in Methods. ns, not significant. Bars and error bars, mean values and s.d. of three biological replicates. ** P <0.01, **** P <0.0001, Student's t -test. **d**, Flow cytometry analysis of ROS in HMLER CD24^{low} cells treated with Sal or AM5 (0.5 μ M) for 72 h +/- DFO (10 μ M). **e**, Quantification of cell viability measured by flow cytometry using Annexin V-FITC and PI fluorescence. HMLER CD24^{low} cells were treated with Sal or AM5 (0.5 μ M) for 72 h. ns, not significant. Bars and error bars, mean values and s.d. of three biological replicates. *** P <0.001, **** P <0.0001, Student's t -test. **f**, Photographs of methanolic solutions of the indicated small molecules +/- iron(II). **g**, Schematic illustration of the fluorogenic reduction of RhoNox-1 with iron(II) and corresponding quantification. Chemical reactions were performed as described in Methods. **h**, Schematic illustration of Sal-induced cell death. Drugs highlighted in red can induce iron depletion. Drugs highlighted in purple can protect cells from Sal-induced cell death. CA, CA-074; DFO, deferoxamine; Fer-1, Ferrostatin-1; FT, ferritin; NAC, *N*-acetyl cysteine.



Supplementary Figure 17 | Preferential uptake of transferrin by ALDH⁺ iCSCL-10A2 CSCs. **a**, Flow cytometry analysis of Alexa-647-TF uptake after 30 and 120 min treatment of ALDH⁺ iCSCL-10A2 cells. **b**, Quantification of **a**. Data points and error bars, mean values and s.d. of two biological replicates. ** $P < 0.01$, *** $P < 0.001$, Student's *t*-test.